Wing morphology of a new Cretaceous praying mantis solves the phylogenetic jigsaw of early-diverging extant lineages

ALEXANDRE V. DEMERS-POTVIN[1] , HANS C.E. LARSSON[1],
MARIO COURNOYER[2] and OLIVIER BÉTHOUX[3]

[1]Redpath Museum, McGill University, Montréal, Canada, [2]Musée de paléontologie et de l'évolution, Montréal, Canada and [3]Centre de Recherche sur la Paléontologie – Paris (CR2P), Sorbonne Université, MNHN, CNRS, Paris, France

Abstract. The extremely derived morphology and behaviour of extant praying mantises combined with a scarce record of fossil relatives introduce significant challenges to tracing their evolution from Palaeozoic stem-dictyopterans. Extant members of Chaeteessidae, Mantoididae and Metallyticidae could be invaluable to resolving the mantodean tree, yet their inclusion in phylogenetic analyses led to conflicting hypotheses due to their highly disparate respective morphologies. In this contribution, we present *Labradormantis guilbaulti* **gen. et sp.n.**, a new fossil species described from both fore- and hind-wing imprints discovered in the Redmond Mine locality (Late Cretaceous, Cenomanian, Redmond Formation; Labrador, Canada). The examination of its hind-wing AA2* supports the hypothesis that this structure, unique to Chaeteessidae among extant mantises, is a true vein and that its occurrence represents a plesiomorphy for Mantodea. A parsimony analysis including newly coded wing-related characters further established that *L. guilbaulti* **gen. et sp.n.** displays a unique combination of plesiomorphic and apomorphic character states that situates it within the extinct family Baissomantidae. This dataset resolved the phylogenetic relationships of early-diverging extant lineages as (Chaeteessidae (Mantoididae (Metallyticidae, Artimantodea))), and suggested that the Eocene *Lithophotina floccosa* Cockerell might be a close relative of extant metallyticids. It also indicated a trend towards increased modularity within mantis fore-wings, in contrast with a trend towards increased morphological integration in their hind-wings, both of which are potentially associated with improved flight performance for modern mantises. This study emphasizes the importance of fossils for resolving phylogenetic relationships and for introducing transitional phenotypes to infer ancient evolutionary trends of extant derived clades.

Introduction

Mantodea as a whole displays a morphological disparity comparable with that of many more speciose insect orders (Ehrmann, 2002; Brannoch *et al.*, 2017; Wieland, 2013). The vast majority of its constituent species (ca. 2500) belong to Artimantodea, commonly referred to as 'praying mantises' (Svenson & Whiting, 2009; Wieland & Svenson, 2018), a group that probably diversified during the Cretaceous Terrestrial Revolution. Among other features, these insects are characterized by highly specialized hunting strategies, involving sophisticated camouflage (Svenson & Whiting, 2004; Svenson *et al.*, 2015, 2016; Schwarz & Roy, 2019; Svenson & Rodrigues, 2019) and prey capture adaptations on the head, forelegs and prothorax (Loxton & Nicholls, 1979; Wieland, 2013; Brannoch *et al.*, 2017; Rivera & Callohuari, 2019).

Both molecular- and morphology-based analyses have consistently recovered Blattodea as the nearest living relatives of Mantodea (Evangelista, et al., 2019b; Grimaldi & Engel, 2005; Klass & Meier, 2006; Legendre *et al.*, 2015; Misof *et al.*, 2014;

Correspondence: Alexandre Demers-Potvin, Redpath Museum, McGill University, 859 Sherbrooke St. W., H3A 0C4, Montréal, Canada. E-mail: alexandre.demers-potvin@mail.mcgill.ca

Ragge, 1955; Smart, 1951, 1956; Wipfler *et al.*, 2019b). However, within Mantodea, the evolutionary sequence leading to the highly speciose and disparate artimantodeans has long been debated. Multiple studies have recovered the species-poor Mantoididae, Chaeteessidae and Metallyticidae (thereafter 'MCM' taxa) as successive sister groups to Artimantodea (Fig. 1). The MCM taxa indeed are far more 'cockroachoid' than the true 'praying mantises'. Notably, they bear raptorial forelegs that retain an important cursorial function, a trait lost in Artimantodea (Wieland, 2008, 2013). This feature aside, MCM species display extremely disparate morphologies, each with a unique combination of traits. For example, whereas the wings of both chaeteessids and metallyticids are reminiscent of those of blattodeans, mantoidids have a wing venation simpler than any other found in the order (Agudelo, 2014; Brannoch *et al.*, 2017: Figs 4, 5; Smart, 1956). At the same time, metallyticids display a unique metallic colouration on their fore-wings and body throughout their ontogeny, as well as highly derived leg spination and phallomere characters putatively homologous to those of artimantodeans (Wieland, 2008, 2013; Schwarz & Roy, 2019). Chaeteessids retain spines on their meso- and metathoracic legs as in blattodeans, but concurrently display a range of apomorphies such as a sharply curved fore tibia with a highly reduced tibial spur (Wieland, 2013). In addition, Chaeteessidae is the only extant mantodean clade to possess a sclerotized line running almost in superimposition to the folding line of the hind-wing. Its origin has been debated in the literature: on one hand, it has been identified as a genuine vein, namely '1V', also present in Blattodea and therefore representing a plesiomorphy within Mantodea (Smart, 1951, 1956). On the other, it has been identified as an intercalary between the anteriormost veins of the anal sector unique to Chaeteessidae ('Iaa$_1$-aa$_2$' in Brannoch *et al.*, 2017), thus representing a synapomorphy for this clade.

Expectedly, the widely divergent morphologies of the MCM taxa have led to a variety of hypotheses on their phylogenetic relationships (Fig. 1). An unresolved polytomy was obtained in a morphology-based investigation that included fossils (Grimaldi, 2003; Fig. 1A). A (Mantoididae (Chaeteessidae (Metallyticidae + Artimantodea))) topology (Fig. 1B) was obtained by Klass & Meier (2006) on the basis of male genitalia. A molecular-based phylogeny recovering Chaeteessidae and its sister group as most early-diverging lineages, followed by Mantoididae and its sister group, with Metallyticidae either sister to Artimantodea or nested within the latter, was obtained by Svenson & Whiting (2009) (Fig. 1C). Based on an extensive morphological character matrix, Wieland (2013) also recovered Chaeteessidae as sister group of the remaining extant mantodeans, but with Mantoididae as sister to Artimantodea (instead of Metallyticidae) (Fig. 1D). In contrast, Legendre *et al.* (2015) found MCM taxa scattered throughout various artimantodean taxa (Fig. 1E). Finally, a recent account provided another distinct hypothesis, differing from that of Wieland (2013) by the respective positions of Mantoididae and Metallyticidae, the latter clade sister to Artimantodea (Schwarz & Roy, 2019; Fig. 1F). This exhaustive review highlights a general uncertainty about the identity of the most ancestral extant taxon within Mantodea and the sister group to the highly disparate Artimantodea.
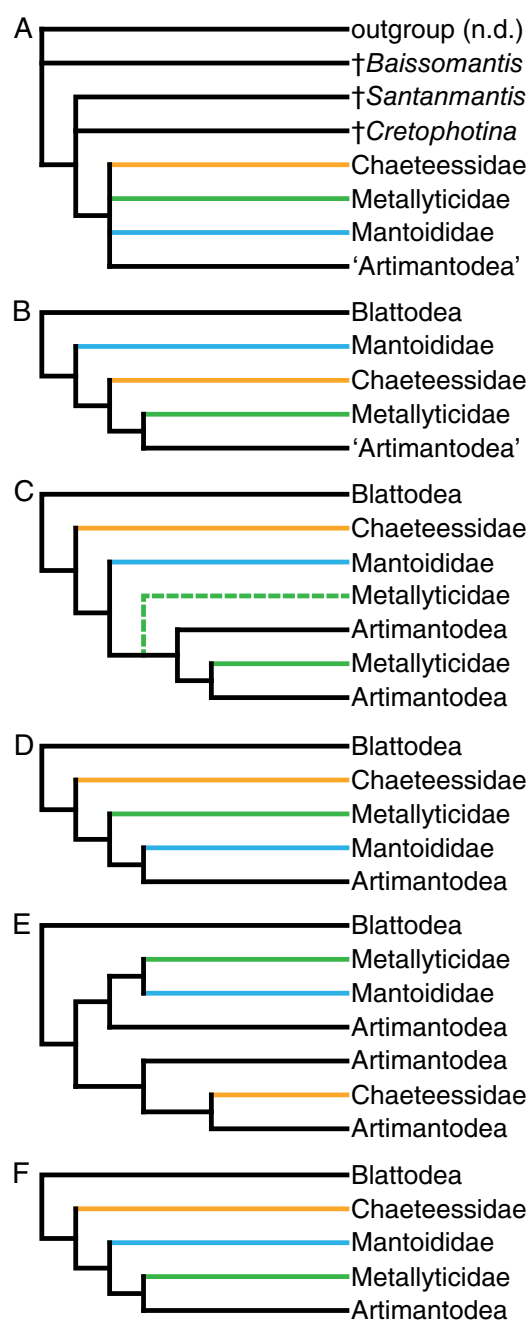

Fig. 1. Phylogenetic hypotheses for basal relationships among Mantodea. (A) Grimaldi (2003), morphology-based parsimony analysis, unordered majority-rule consensus, including fossils (in italics). (B) Klass & Meier (2006), morphology-based parsimony analysis, most parsimonious tree, crown-group only. (C) Svenson & Whiting (2009), molecular-based maximum-likelihood analysis. (D) Wieland (2013), morphology-based parsimony analysis, strict consensus with characters weighted, crown-group only. (E) Legendre *et al.* (2015), molecular-based analysis. (F) Schwarz & Roy (2019), total-evidence phylogenetic frame, crown-group only. Artimantodea written in brackets for phylogenies preceding the introduction of this taxon by Svenson & Whiting (2009). [Colour figure can be viewed at wileyonlinelibrary.com].

The fossil record of Mantodea was also considered as an additional line of inquiry, yet it proved equally frustrating. Among the ca. 26 well-ascertained ancient mantodeans, only a few mature Cretaceous specimens, such as *Ambermantis wozniaki* Grimaldi and *Santanmantis axelrodi* Grimaldi, display key characters across the entire body, including forelegs, pronotum and wings. Indeed, most Cretaceous mantodeans are represented either by nymphs, preserved in amber, or by isolated wings, which makes the tracing of certain character transitions challenging (Gratshev & Zherikhin, 1993; Grimaldi, 2003; Lee, 2014; Delclòs *et al.*, 2016; Li & Huang, 2018). To date, this documentation provided limited insights on the sequence of character state acquisition of critical structures, including raptorial forelegs (Hörnig *et al.*, 2013, 2017; Dittmann *et al.*, 2015).

In this study, we report the discovery of a new Cretaceous stem-mantodean species, *Labradormantis guilbaulti* **gen et sp.n.** The character state combination it displays is unique and provides decisive insight on the debate surrounding the evolution of the mantodean body plan.

Materials and methods

Institutional abbreviations and morphological terminology

AMNH, American Museum of Natural History, New York City, U.S.A.; IWC OB, Insect Wing Collection (Olivier Béthoux); MNHN, Muséum national d'histoire naturelle, Paris, France; MPEP, Musée de paléontologie et de l'évolution (Palaeontology samples), Montréal, Canada; OUMNH, Oxford University Museum of Natural History, Oxford, United Kingdom; PIN, Palaeontological Institute, Moscow, Russia; RU-DE-IWO, Rutgers University Entomology Museum (D. Evangelista collection, Iwo Jima), Newark, U.S.A.; UCM, University of Colorado Museum of Natural History, Boulder, U.S.A.

The serial wing venation nomenclature proposed by Lameere (1922, 1923), subsequently modified by Kukalová-Peck (1991), discussed by Béthoux (2005) and recently adapted for dictyopterans by Brannoch *et al.* (2017), is largely followed in the description herein. Wing venation abbreviations are repeated here for convenience, together with corresponding colour coding: AA1, first anterior analis; AA2, second anterior analis; CuA, anterior cubitus (green); CuP, posterior cubitus (green); M, media (red); R, radius (blue); RA, anterior radius (blue); RP, posterior radius (blue); ScP, posterior subcosta. A portion of a vein is indicated by '*p*', accounting for '*partim*' ('in part' in Latin). Inferred portions of venation are represented in light grey.

According to Brannoch *et al.* (2017), we refer to the hinge along which the plicatum folds as 'ppa' (plica prima anterior; orange dashed line). The thin slit occurring along the anterior side of M (i.e. between R/RA + RP and M) is designated as 'median flexion line' (Wootton, 1979). The term 'AA2*', the first vein of the second anterior analis, will be described in greater detail (see Discussion).

Material and geological setting

The two specimens which are the focus of the current contribution were collected by the third author at an exposure of the Redmond Formation in the Redmond no. 1 Mine, an abandoned iron ore mine located in Labrador, Canada, near the town of Schefferville, Québec, Canada (Dorf, 1959; Demers-Potvin & Larsson, 2019). Most plant and insect fossils discovered at this locality were found among float during the last decade, after the red argillite bed that preserved them was brought out of geological context due to mining activities. The few insects described from the Redmond Mine locality are a snakefly (Alloraphidiidae, see Carpenter, 1967), an antlion (Myrmeleontidae, see Rice, 1969), a stem-phasmatodean (Rice, 1969), a termite (Hodotermitidae, see Emerson, 1967), a protocoleopteran (Labradorocoleidae, see Ponomarenko, 1969), and a recently described hairy cicada (Hemiptera: Tettigarctidae, see Demers-Potvin *et al.*, 2020b). Additionally, undescribed articulated mayfly nymphs and water beetles were recovered, further indicating a lacustrine depositional setting for the formation (Demers-Potvin & Larsson, 2019). Stratigraphic correlation was derived from its leaf assemblage and suggests a Late Cretaceous, probably Cenomanian, age (Blais, 1959; Dorf, 1959, 1967). The mixed forest around this ancient lake would have experienced a warm temperate climate (mean annual temperature ca. 15°C) at a palaeolatitude of ca. 49°N (Demers-Potvin & Larsson, 2019).

The holotype of the newly described species (MPEP1157.6) was recovered during a joint expedition between the Redpath Museum and the Musée de paléontologie et de l'évolution (MPE) in August 2018. It consists of two incomplete fore-wings (as negative imprints) and two fragmentary legs. The paratype (MPEP702.11) was found in August 2013 during an expedition directed by the MPE. Each of its two sides preserves two almost complete hind-wings, the nearly complete clavus of a fore-wing, the metathorax and isolated leg segments. The specimens are deposited in the Palaeontology collection of the MPE.

Data acquisition

Photographs reproduced on Figs 2A, C, 4A, B, 5A, F were extracted from Reflectance Transformation Imaging (RTI) files. These were built by AVD-P out of sets of photographs in order to facilitate remote observation and to obtain images under ideal lighting conditions. The original sets of photographs were taken using a Portable Light Dome involving a Canon EOS 5D Mark III digital camera equipped with a Canon MPE-65 macro lens (Canon, Tokyo, Japan). Individual photographs from a set were then processed using Adobe Camera Raw and Adobe Photoshop CC 2019 (Adobe Systems, San Jose, CA, U.S.A.). They were then compiled into an RTI file using the RTI Builder software v. 2.0.2 (freely available under GNU license, using the HSH fitter; and see Béthoux *et al.*, 2016; Reflectance Transformation Imaging (RTI), 2019). This process was repeated for four RTI files in total: the holotype (MPEP1157.6) was documented by a complete specimen view (Appendix 1.1), and closeups of the stigma of each fore-wing; the paratype

Table 1. List of stem-dictyopteran, blattodean and mantodean taxa included in the phylogenetic analysis of *Labradormantis guilbaulti* **gen. et sp.n.** Specimen numbers are provided in cases where additional data were obtained and consulted by the authors

Taxon	Age	Locality (for fossils)	References
Labradormantis guilbaulti **gen. et sp.n.**	Late Cretaceous (Cenomanian)	Redmond no.1 Mine (Redmond Formation), Newfoundland and Labrador, Canada	This study
Baissomantis picta Gratshev & Zherikhin, 1993	Late Cretaceous (Campanian)	Baissa, Zaza Formation, Transbaikalia, Russia	Gratshev & Zherikhin (1993: Fig. 3A–C); Grimaldi (2003: Fig. 5A); PIN 1989/2490, PIN 1668/1645 (photographs)
Buboblatta vlasaki Evangelista *et al.*, 2019a	Recent	–	Evangelista *et al.* (2019a: Figs 2, 3)
Chaeteessa spp.	Recent	–	Brannoch *et al.* (2017: Fig. 4D–F); Klass & Meier (2006: p. 14); Smart (1956: Fig. 1); Wieland (2013: Figs 68, 100, 110, 148–9, 277, 302); OUMNH-4566 (photographs)
Crenocticola burmanica Li & Huang, 2020	Late Cretaceous (Cenomanian)	Hukawng Valley, Kachin, Myanmar	Li & Huang (2020: Figs 1–3)
Cretophotina tristriata Gratshev & Zherikhin, 1993	Late Cretaceous (Campanian)	Baissa, Zaza Formation, Transbaikalia, Russia	Gratshev & Zherikhin (1993: Fig. 1A–C); Grimaldi (2003: Figs 5B, C, 6A); PIN 1989/2488 (photographs)
Deroplatys lobata Guérin-Méneville, 1838	Recent	–	Béthoux & Wieland (2009: Fig. 12E, F); Wieland (2013)
Ectobius sp.	Recent	–	IWC OB 103, IWC OB 539 (direct observation)
Lithophotina floccosa Cockerell, 1908	Eocene (Priabonian)	Florissant Formation, Colorado, U.S.A.	Sharov (1962: Fig. 1); UCM IP 4527 (photographs)
Mantis religiosa Linnaeus, 1758	Recent	–	Brannoch *et al.* (2017: Fig. 5D–F); Wieland (2013); IWC OB 78–87, IWC OB 89–91 (direct observation)
Mantoida maya Saussure & Zehntner, 1894	Recent	–	Brannoch *et al.* (2017: Fig. 5A–C); Klass & Meier (2006: p. 14); Wieland (2013: Figs 70, 101, 114, 150–4, 258–0, 304, 349)
Metallyticus splendidus Westwood, 1835	Recent	–	Brannoch *et al.* (2017: Fig. 4A–C); Klass & Meier (2006: p. 14); Wieland (2008: Figs 1, 2, 6–13); Wieland (2013: Figs 303, 353); IWC OB 193, IWC OB 194
Miobantia fuscata Giglio-Tos, 1917	Recent	–	Scherrer (2014: Figs 4, 11C, 14D, 16C, 17E)
Molytria sp.	Recent	–	Cui *et al.* (2018: Fig. 2A, B)
Nyctibora sp.	Recent	–	Klass & Meier (2006); RU-DE-IWO-0428
Periplaneta americana Linnaeus, 1758	Recent	–	Klass & Meier (2006: p. 14); Smart (1951): Figs 1, 2); Schneider (1977a: Tafel I); Schneider (1977b: Figs 1–6, Tafel I, II); Wieland (2013: Figs 81, 99, 145–7, 255–7, 301)
Phyloblatta gaudryi Agnus, 1903	Late Pennsylvanian (Gzhelian)	Commentry Shales Formation, Allier, France	Béthoux *et al.* (2011: Figs 1-3); MNHN.F.R51255; MNHN.F.R51480; MNHN.F.R51570; MNHN.F.R51526; MNHN.F.R51468; MNHN.F.R51469; MNHN.F.R51557 (photographs)
Phyloblatta occidentalis Scudder, 1890	Late Pennsylvanian (Kasimovian-Gzhelian)	El Menisla and Oued Issene formations, Souss Basin, Morocco	Belahmira *et al.* (2019: Figs 7(1), 8–11)
Qilianiblatta namurensis Zhang *et al.*, 2013	Early Pennsylvanian (Namurian)	Xiaheyan, Tupo Formation, Ningxia, China	Zhang *et al.* (2013: Fig. 3); Guo *et al.* (2013: Fig. 1); Wei *et al.* (2013: Figs 1, 2)
Santanmantis axelrodi Grimaldi, 2003	Early Cretaceous (Aptian)	Crato Formation, Brazil	Grimaldi (2003: Figs 16, 17, 20–24); Hörnig *et al.* (2013: Fig. 2); Hörnig *et al.* (2017: Figs 1, 3); AMNH-1956, AMNH-1957 (direct observation)

(MPEP702.11) was documented by a complete specimen view of the part (MPEP702.11a, see Appendix 1.2) and counterpart (MPEP702.11b, see Appendix 1.3), and a closeup of the folding line between remigium and plicatum in the best-preserved hind-wing base (MPEP702.11b, see Appendix 1.4). These files are provided along with viewer software and instructions in Appendix S1 (Demers-Potvin *et al.*, 2020a). Measurements were performed using FIJI (Schindelin *et al.*, 2012).

Draft drawings were made by AVD-P and OB with a microscope equipped with a camera lucida (Zeiss SteREO Discovery V8 stereomicroscope equipped with a pair of W-PL 10×/23 eye pieces, a Plan Apo S 1.0× FWD objective; all Zeiss, Jena, Germany). The drawings were finalized using Adobe Illustrator CC 2019 (Adobe Systems, San Jose, CA, U.S.A.) using both draft drawings and photographs. For comparative purposes, photographs of a possible extinct relative, *Baissomantis picta* Gratshev & Zherikhin, were taken at different light orientations, in dry conditions and in ethanol.

Phylogenetic analysis

The phylogenetic position of the new fossil species within Dictyoptera was tested by AVD-P and OB using morphological data and a selection of relevant taxa (Table 1). Some species of stem-mantodeans were not considered for this analysis. *Arvernineura insignis* Piton and *Cretophotina santanensis* Lee were not retained because of uncertain interpretations of the corresponding material, nor were complete mature taxa such as *A. wozniaki* or *Burmantis hexispinea* Li & Huang, due to insufficient data on their wing venation.

The inclusion of *Baissomantis maculata* Gratshev & Zherikhin was attempted, but it consistently led to a polytomy between all Cretaceous stem-mantodeans, blattodeans and crown-mantodeans. This seemed to be caused by the failure to locate a stigma (possibly obscured by dark dense spots) combined with the presence of a branched AA1. The occurrence of AA2* could not be assessed in *Ba. maculata* based on the available data. Given that the species newly described herein is, on one hand, closely related to *Baissomantis* spp. and, on the other, more completely documented than *Ba. maculata*, it was considered unnecessary to include the latter.

As for Blattodea, our selection aimed to broadly cover the taxonomic range of the group and the variety of known wing morphologies. The selection was also driven by data availability on characters relevant to the placement of the new fossil (i.e. wing venation). Three Pennsylvanian 'roachoids' for which hind-wings are at least partly documented (in addition to fore-wings) were also selected. Among them, *Qilianiblatta namurensis* Zhang *et al.* was set as the outgroup, owing to the presence of well-differentiated RA and RP veins in the fore-wing of this species. This character state is widely regarded as plesiomorphic within Blattodea/Dictyoptera (Pruvost, 1919; Laurentiaux-Vieira & Laurentiaux, 1980; Schneider, 1984; Guo *et al.*, 2013).

Since the recently erected order Alienoptera has been proposed as an extinct sister taxon of Mantodea (Bai *et al.*, 2016; Wipfler *et al.*, 2019a), the inclusion of one of its members was considered. However, the proposed conjecture of wing venation homology for the hind-wing (Kočárek, 2019) requires a revision, since the vein identified as RP is most likely M (then MA_1, MA_2 and MP together forming the CuA system; etc.). This uncertainty, coupled with the severe reduction of the fore-wing in this order, prevented us from including any alienopteran in our analysis.

A morphological character matrix was assembled in Mesquite v.3.6 (build 917) (Maddison & Maddison, 2018). It contains 61 morphological characters, 22 of which pertain to wing morphology (see Appendices 2.1, 2.2). The data were mostly modified from that of Wieland (2013) covering extant Mantodea. Only 43 of the original 152 characters were relevant for the subset of selected extant mantodeans. The coding of some of the retained characters was altered (see Appendix 2.1). We also coded 12 new wing venation characters, including the presence/absence of intercalaries in the fore-wing clavus (char. 10), a character already highlighted by Cui *et al.* (2018) as relevant to distinguish Blattodea from Mantodea. The remaining characters include the branching pattern of the fore-wing's RA + RP (char. 1), the extent of the fore-wing plicatum (char. 8), the shape and location of the stigma in the fore-wing (char. 12), the position of MA (the anterior branch of the media) in the fore-wing (char. 14), the presence/absence of the median flexion line between the fore-wing RA + RP and M (char. 15), the shape of AA2 branches in the clavus (char. 16), the presence/absence of the AA2* in the hind-wing (char. 21), and the number of cell rows between fore-wing branches (char. 22). The coding of the latter characters largely arose from observations of extant blattodean and mantodean wings mounted on slides as part of OB's Insect Wing Collection (IWC OB; see Béthoux & Wieland, 2009 for details on preparation of slides). The dataset was complemented by characters of male genitalia coded by Klass & Meier (2006) that influenced the placement of MCM taxa in previous phylogenetic investigations. Given our species sample, six of these characters proved to be informative (chars. 56–61) and were therefore retained.

A parsimony analysis was performed with PAUP* v.4.0a (build 166) (Swofford, 2002), with all characters unordered and equally weighted. A branch-and-bound search retaining only the most parsimonious trees was executed. Different searches were run under ACCTRAN and DELTRAN optimizations for ambiguous characters following the demonstration that neither of these assumptions should be favoured (Agnarsson & Miller, 2008). The sensitivity of the obtained cladogram was assessed with Bremer, Jackknife and Bootstrap measures of branch support. Bremer support for each clade was calculated by running successive branch-and-bound searches in which the maximum number of steps allowed for retaining trees was constantly raised until all branches were collapsed. The Jackknife was applied with 100 replicates and random deletion of either 5% or 10% of matrix characters, for strict consensus and 50% majority-rule consensus trees. The bootstrap was applied with 100 replicates and resampling of all 61 characters, for strict consensus and 50% majority-rule consensus trees. Consistency and retention indices were calculated for the strict consensus tree
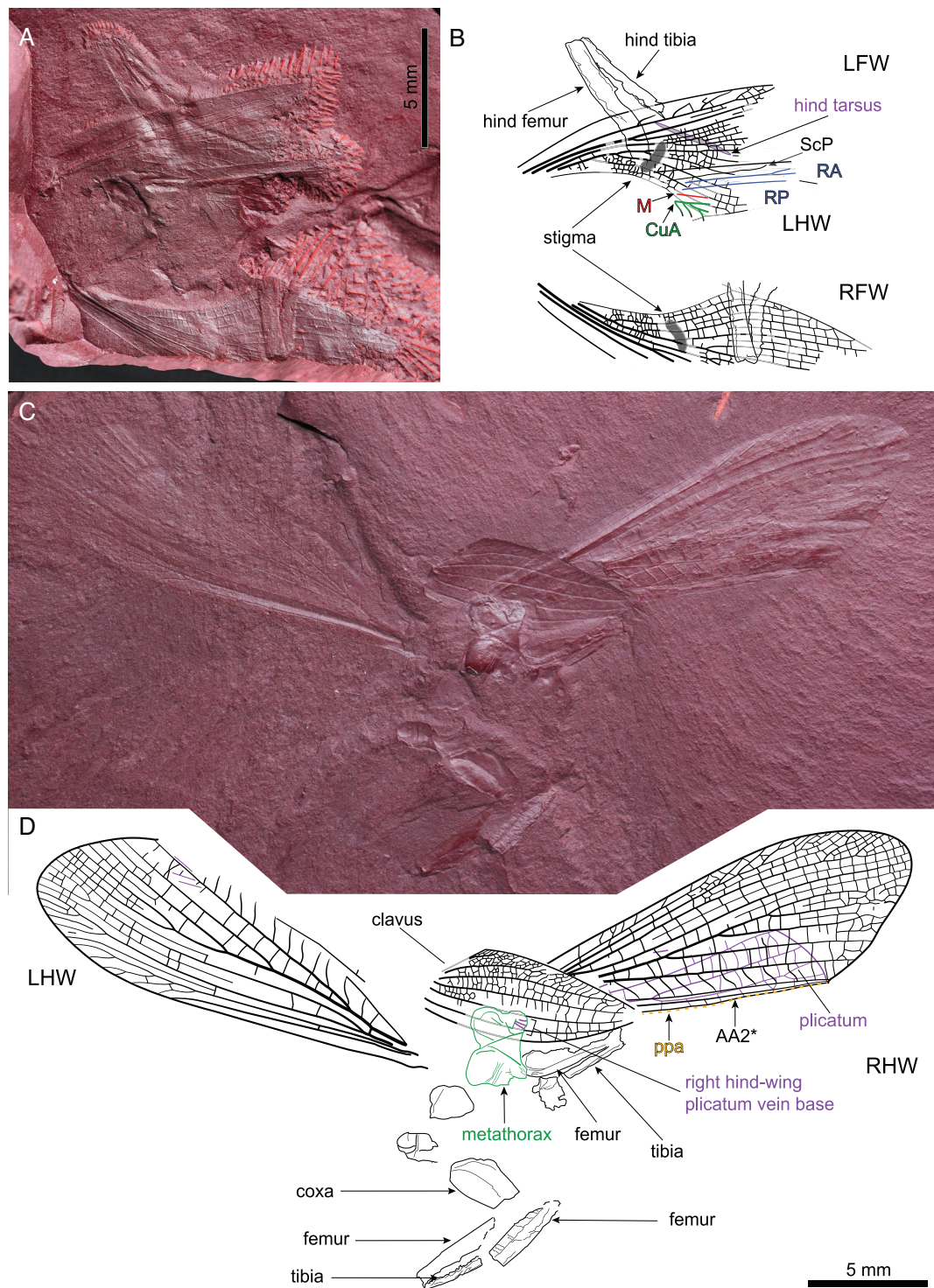
Fig. 2. General habitus of *Labradormantis guilbaulti* **gen. et sp.n.** (Late Cretaceous, Cenomanian, Redmond Formation; Labrador, Canada). (A, B) Holotype, MPEP1157.6, habitus; (A) photograph (light-mirrored; RTI file extract, see Appendix 1.1); (B) interpretative line drawing. (C, D) Paratype MPEP702.11a, habitus; (C) photograph (RTI extract, see Appendix 1.2); (D) interpretative line drawing. Abbreviations and colour-coding: LFW, left fore-wing; LHW, left hind-wing; RFW, right fore-wing; RHW, right hind-wing; AA2*, first vein of second anterior analis; CuA, anterior cubitus (green); M, media (red); RA, anterior radius (blue); RP, posterior radius (blue); ScP, posterior subcosta; stigma, dark grey; ppa, plica prima anterior (orange, dashed line). [Colour figure can be viewed at wileyonlinelibrary.com].

without measures of support, as well as the 50% majority-rule consensus tree with Bootstrap and the 50% majority-rule consensus tree with 5% Jackknife deletion. These indices were also calculated for each individual character in each of these three consensus trees (see Appendix 2.1).

Results

Systematic palaeontology

This section focuses on the description of a new species of fossil mantodean. We provide documentation of the complete material (Fig. 2), wing reconstructions (Fig. 3) and details of fore- and hind-wing structures relevant for systematic placement (Figs 4, 5, respectively).

Order Mantodea Burmeister, 1838
Family Baissomantidae Gratshev & Zherikhin, 1993
Emended diagnosis. RA + RP branching into distinct RA and RP (possibly RA*p* and RA*p* + RP) longitudinal veins basad of wing mid-length, each of which remain unbranched for a long distance, at least until they run apicad of the apical end of ScP. This emendation of the original diagnosis of Baissomantidae was caused by the inclusion of the new genus to this family.

Composition. The family includes the genera *Baissomantis* (including *Baissomantis picta* Gratshev & Zherikhin, 1993 and *Baissomantis maculata* Gratshev & Zherikhin, 1993; see original descriptions and Grimaldi, 2003) and *Labradormantis* **gen.n.**

Genus †*Labradormantis* gen.n.
Zoobank LSID: urn:lsid:zoobank.org:act:57E28952-AB78-478C-B495-3AAD3E730D7F

Type species. †*Labradormantis guilbaulti* **sp.n.**, designated here.

Etymology. Derived from the continental region of the Canadian province of Newfoundland-and-Labrador, where the Redmond no.1 Mine is located.

Diagnosis. By monotypy, as for the type species.

†*Labradormantis guilbaulti* sp.n.
Zoobank LSID: urn:lsid:zoobank.org:act:C6BE013F-635F-422C-95B0-48376552619A

Material. Holotype, MPEP1157.6, consisting in two incomplete fore-wings, each with their clavus lost, along with two fragmentary legs. Paratype, MPEP702.11 (part and counterpart), consisting in two almost complete hind-wings, the almost complete clavus of a fore-wing, the metathorax and isolated leg segments. Clavus more complete in the part; metathorax more complete in the counterpart.

Etymology. The specific epithet refers to Jean-Pierre Guilbault, co-founder of the MPE, in honour of his contribution to the MPE's first expedition to the Redmond Mine and of his ongoing contributions to the advancement of this museum.

Locality and horizon. Redmond no.1 Mine located at coordinates 54°41′N and 66°45′W, Newfoundland-and-Labrador, Canada, 16 km south southeast of Schefferville; Redmond Formation, Late Cretaceous, Cenomanian (93.9–100.5 Ma).

Diagnosis. In fore-wing, stigma ellipsoidal, slightly curved (as opposed to a forming a strap-shaped patch, as in *Baissomantis*). In hind-wing, intercalary vein in the RP–M area arising basad of the first fork of RA (as opposed to arising apicad of the first fork of RA, as in *Baissomantis*).

Description. Holotype (MPEP1157.6; Figs 2A, B, 3A*partim*, 4A, B; RTI file in Appendix S1; extended description in Appendix 3.1): **Fore-wings**: ScP reaching the anterior wing margin near the second third of wing length, anteriorly pectinate, with four, somewhat distant sigmoid branches separated by cross-veins; area between anterior wing margin and ScP more than four times as wide as ScP-RA area near wing base; RA + RP slightly bent posteriorly in basal third of wing length, then forking into well-differentiated simple and subparallel RA and RP; occurrence of an intercalary in the apical part of the RA–RP area; M first fork apicad of RA + RP fork; median flexion line conspicuous in both fore-wings (Fig. 4A, B; and corresponding RTI in Appendix S1); CuA posteriorly pectinate, with five preserved branches, basal most branches sigmoid; stigma present, forming an ellipsoidal, smooth area, located apicad of RA + RP first fork but basad of M fork (Figs 2A, B; 4A, B, corresponding RTI in Appendix S1); two cell rows formed by intercalaries between each vein in apical CuA area. **Left hind-wing**: only antero-basal area preserved; ScP reaching the anterior wing margin; as preserved, RA with an apical fork, RP simple, M simple; CuA with a main fork and posterior veinlets. **Legs**: two articulated leg fragments preserved, each of them seemingly composed of a hind femur attached to a hind tibia.

Paratype (MPEP702.11; Figs 2C, D, 3A*partim*, B, 5A, B, E, F; three RTI files in Appendix S1; extended description in Appendix 3.1): **Fore-wing**: isolated clavus almost completely preserved, with six subparallel veins, including CuP; length ca. 8 mm, width ca. 4 mm at widest point; AA1 simple, reaching CuP apically; course of AA2 veins ranging from concave to sigmoid from anterior to posterior margin; development of regular pectinate pattern with sigmoid trajectory in apical (posterior) corner. **Hind-wings**: ScP straight, reaching anterior margin past wing mid-length; R forking into RA and RP very close to wing base; RA anteriorly pectinate, with five main branches and six terminal branches; intercalaries clearly defined between ultimate branches of RA, in the RA–RP area, and between branches of RP; RP–M intercalary originating past the basal third of wing length; M closely approximating R near wing base, fused with RP for a short distance, diverging from it past the arculus; M simple (right wing) or forked close to apex (left wing); arculus conspicuous, thicker than other cross-veins; CuA posteriorly pectinate, with five branches reaching margin, and sigmoid veinlets in the basal part of the CuA–CuP area; two cell rows formed by intercalaries between each vein in apical wing area; simple AA1 and ppa running subparallel to CuP, converging towards margin; AA2* conspicuous, forming a thick line running along ppa, with preservation state similar to that of other longitudinal veins (Fig. 5A, F, corresponding RTI in Appendix S1); ppa running posterior to AA2* basally then running superimposed to it apically; two AA1–AA2*
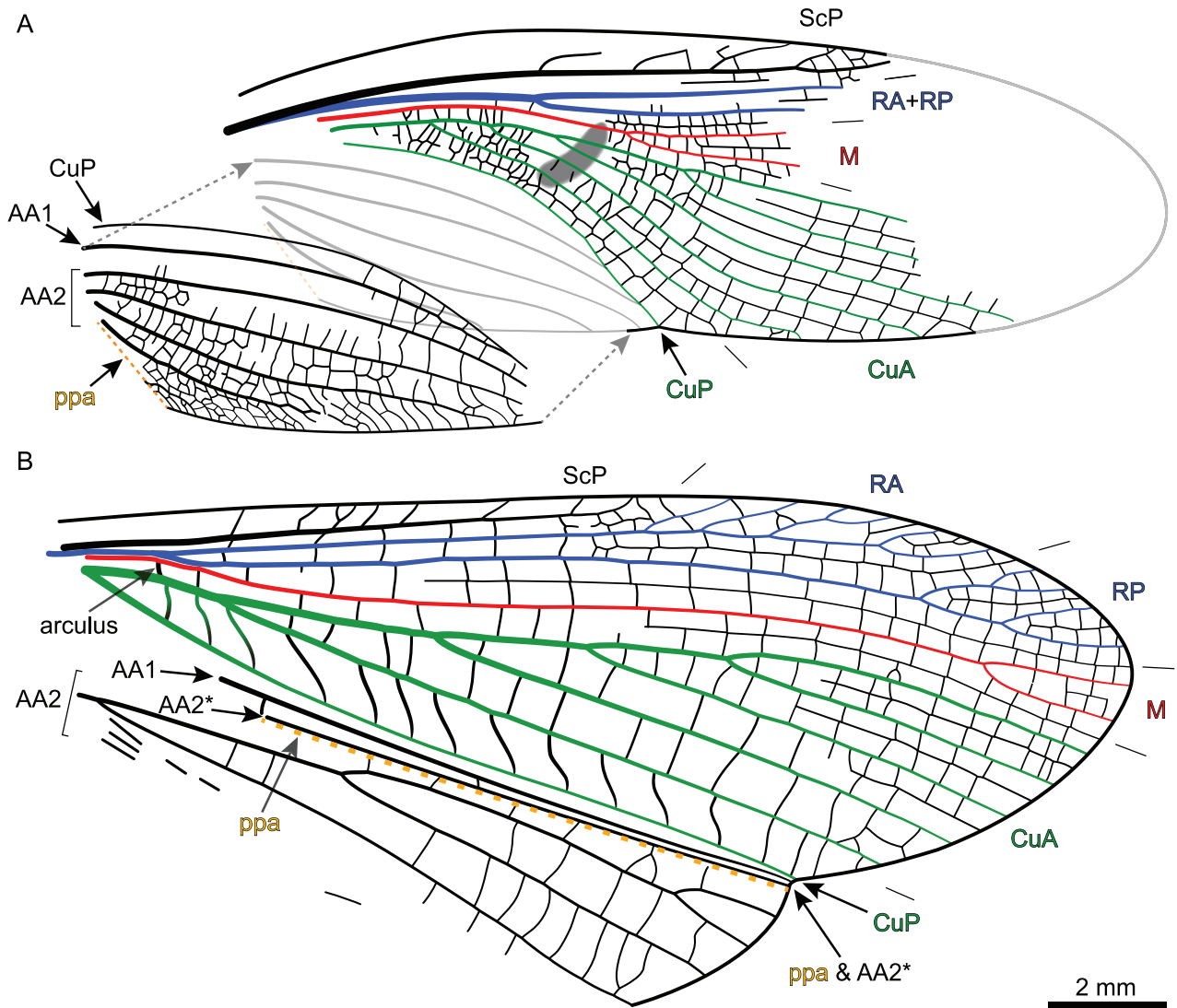
Fig. 3. Reconstruction of wing venation in *Labradormantis guilbaulti* **gen. et sp.n.** (A) Fore-wing reconstruction based on two remigia on MPEP1157.6 (Fig. 2A, B) and on clavus preserved on MPEP702.11 (Fig. 2C, D; in gray, reduced at ca. 85% of its size), apex based on material of *Baissomantis picta* Gratshev & Zherikhin. (B) Hind-wing reconstruction based on two almost complete wings on MPEP702.11, plicatum presented in unfolded state. Abbreviations and colour-coding: AA1, first anterior analis; AA2, second anterior analis; AA2*, first vein of second anterior analis; CuA, anterior cubitus (green); CuP, posterior cubitus (green); M, media (red); RA, anterior radius (blue); RP, posterior radius (blue); ScP, posterior subcosta; stigma, dark gray; ppa, plica prima anterior (orange, dashed line). *Note*: hind-wing basalmost CuA-CuP 'cross-veins' colour-graded to acknowledge possibility that they might instead be true veins (still considered cross-veins in the phylogenetic analysis). [Colour figure can be viewed at wileyonlinelibrary.com].

cross-veins visible; plicatum folded along ppa (right hind-wing; Figs 2C, D, 5A, B, E, F); only anterior part of plicatum visible underneath remigium, no vannal folds visible; four branches of AA2 visible, one forking point just basad of plicatum margin; bases of three veins visible near the posterior right corner of metanotum, probably belonging to the right hind-wing plicatum. **Metanotum**: almost completely preserved, ca. 3.1 mm wide, lacking posterior edge; two anterior lobes complete, each ca. 1.9 mm long, 1.5 mm wide; triangular scutellum visible between them. **Legs**: six segments poorly preserved.

Comments. A justification for the assignment of the two type specimens to the same species is provided in Appendix 3.1.1.

Labradormantis guilbaulti **gen. et sp.n.** can be confidently assigned to Baissomantidae owing to the occurrence of the character state 'RA+RP branching into distinct RA and RP longitudinal veins basad of wing mid-length, each of which remains unbranched for a long distance'. Compared with *Ba. maculata* (for which a hind-wing is documented in addition to a fore-wing), the Redmond Mine species has less-developed posterior-most CuA branches in the hind-wing, and a hind-wing RP–M intercalary arising more basally. Compared with *Ba. picta* (for which only the fore-wing is documented), it has a stigma with an ellipsoidal, slightly curved shape (as opposed to a strap-shaped patch in *Ba. picta*). This unique combination
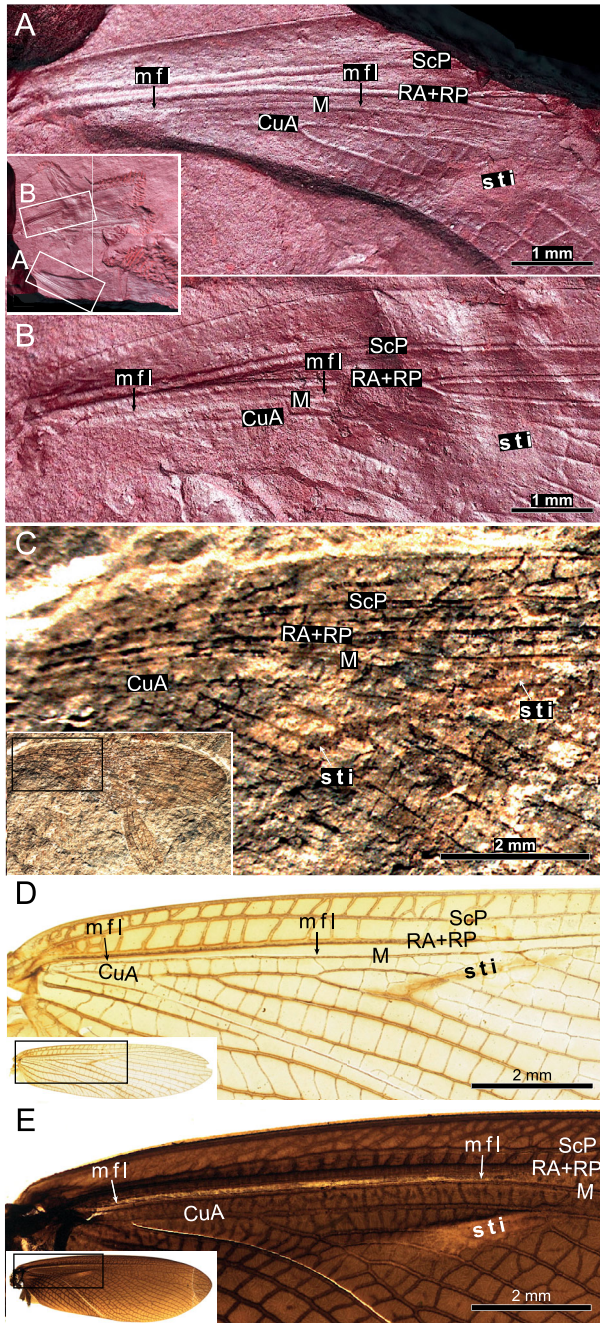
Fig. 4. Photographs of details of stigma and median flexion line in basal half of fore-wing in stem- and crown-mantodeans. (A, B) *Labradormantis guilbaulti* **gen. et sp.n.**, holotype (MPEP1157.6), details located as indicated in middle left inset (RTI file extracts, see Appendix 1.1); (A) right fore-wing (light-mirrored); (B) left fore-wing. (C) *Baissomantis picta* Gratshev & Zherikhin (paratype PIN 1989/2490). (D) *Chaeteessa filata* Burmeister (OUMNH-4566); (E) *Metallyticus splendidus* Westwood (IWC OB 193). Abbreviations: CuA, anterior cubitus; M, media; RA, anterior radius; RP, posterior radius; ScP, posterior subcostal; sti, stigma (both extremities labelled in C); mfl, median flexion line (both extremities labelled; mfl not detected in *Baissomantis* based on available data). [Colour figure can be viewed at wileyonlinelibrary.com].
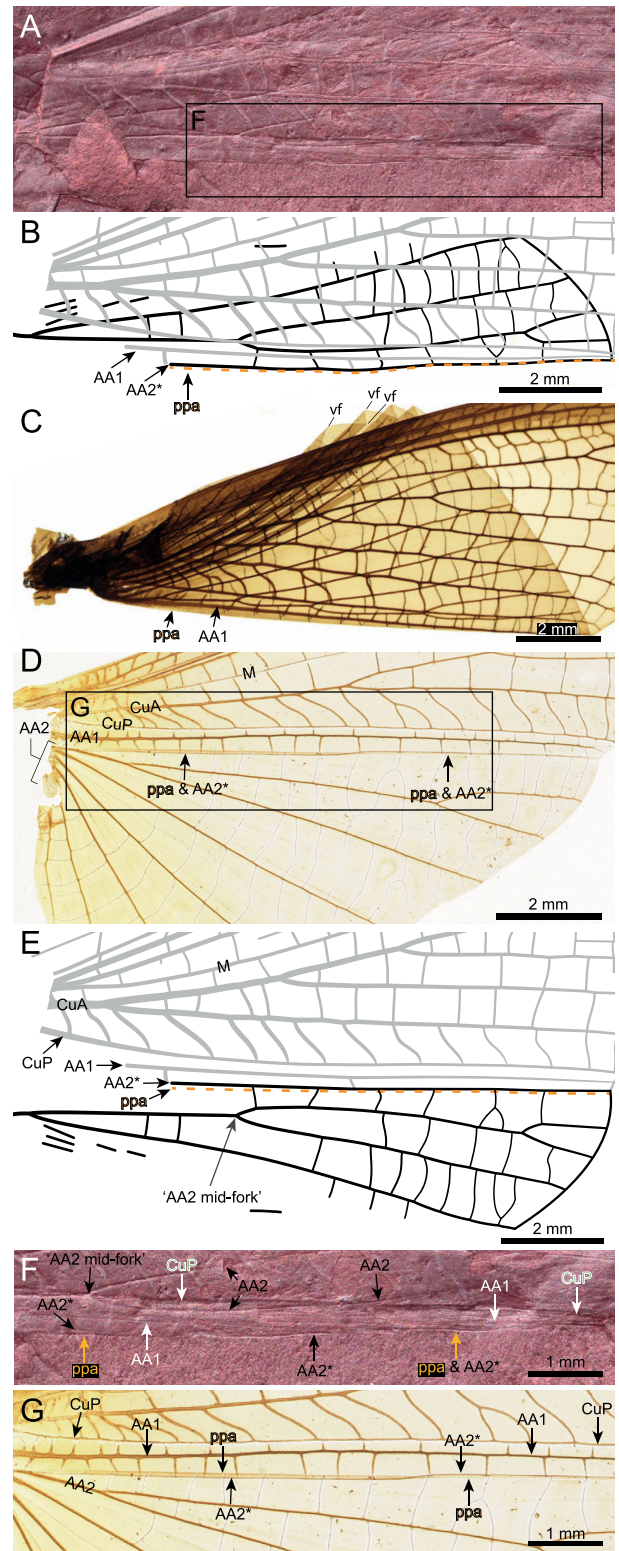
Fig. 5. Legend on next Page [Colour figure can be viewed at wileyonlinelibrary.com].

of traits therefore justifies the erection of a new species and genus.

Phylogenetic analysis

The maximum parsimony analysis yielded 60 equally parsimonious trees with 105 steps (Fig. 6; CI = 0.667, RI = 0.787). As expected, all trees recovered Blattodea and Mantodea as monophyletic groups. Phylogenetic relationships within Mantodea were fully resolved, although Blattodea formed an unresolved polytomy. The consensus tree also supported the monophyly of Eumantodea Grimaldi, which excludes all Cretaceous fossils, and of Artimantodea *sensu* Schwarz & Roy (2019). As expected from the descriptive comparisons above, *Labradormantis guilbaulti* **gen. et sp.n.** was recovered as a sister of *Ba. picta*. This relationship was instrumental to the emendation of the diagnosis for Baissomantidae (see Systematic palaeontology).

Synapomorphies of each major clade relevant to the evolution of mantodean wing morphology are presented in Fig. 6A, B, with schematized drawings representing major transitions in the fore-wing's stigma, plicatum and RA + RP branching pattern at certain nodes (see character list in Appendix 2.1). Within Dictyoptera, node 1 is characterized by the lack of a clear differentiation between RA and RP in the fore-wing, both veins forming a dense comb-like branching instead (Fig. 6B-i). Despite their assignment in the same genus, *Phyloblatta gaudryi* Agnus and *Phyloblatta occidentalis* Scudder were not recovered as sister taxa. Blattodea and Mantodea form a clade (node 2 in Fig. 6A) defined by the presence of a stigma (1) on at least one of the fore-wings, and (2) forming a line crossing CuP (Fig. 6B-ii, iii). Another character state relevant to this node is the number of cell rows not exceeding two between consecutive longitudinal veins in the fore-wing. Blattodea was supported as a monophyletic group based on a fore-wing ScP ending within the proximal quarter of wing length (Fig. 6B-ii), the absence of a transverse folding in the clypeus, and kidney-shaped compound eyes. The occurrence of a stigma on the right fore-wing only (as opposed to both wings in Mantodea) has also been noted (Ross, 2012 among others), although an adaptive function has yet to be proposed for this structure.

Mantodea was recovered as a monophyletic group based on at least one AA2 branch in the clavus with a pronounced sigmoid course, a reduced pronotum (i.e. covering at most the posteriormost part of the head), the presence of raptorial forelegs, and the presence of a tibial spur, among other characters. Within this clade, all Cretaceous fossils included in the analysis were recovered outside Eumantodea, with *Santanmantis* and its sister group being the most early-diverging lineages, *Cretophotina* as an immediate sister group of Eumantodea, and Baissomantidae forming an intermediate clade. *Santanmantis* is sister to a group (node 3 in Fig. 6A) defined, among other characters, by a change in shape and location of the stigma, where it now forms a patch restricted to the fore-wing's remigium (Fig. 6B-iv). Baissomantidae is sister to a *Cretophotina* + Eumantodea clade (node 4 in Fig. 6A) defined by a fore-wing ScP reaching at least two thirds

of total wing length, and a forking point of RA + RP clearly apicad of mid-wing.

Eumantodea was defined by the absence of branches in the hind-wing RA, and a narrow area between the anterior fore-wing margin and ScP. Within Eumantodea, *Chaeteessa* Burmeister is recovered as earlier-diverging than *Metallyticus* Westwood and *Mantoida* Newman, which makes it sister to a clade (node 5 in Fig. 6A) defined by a median flexion line forming a poorly defined, unsclerotized line in the fore-wing, and the absence of AA2* in the hind-wing. Whether a simple, unbranched fore-wing RA + RP represents an apomorphy for this clade (with a reversal for Metallyticidae, displaying a comb-like branching of undifferentiated RA + RP) or a convergence between *Mantoida* and Artimantodea cannot be assessed (Fig. 6B-v). *Mantoida* is recovered as sister to a (Metallyticidae + Artimantodea) clade (node 6 in Fig. 6A) supported by a fore-wing CuP with a sigmoid (as opposed to uniform) curvature, and a short hind-wing ScP ending beyond the apical third of wing length. Metallyticidae, in which *Lithophotina floccosa* is also recovered, is characterized by a comb-like branching of undifferentiated RA + RP in the fore-wing (but see above), AA1 almost or entirely reaching the posterior fore-wing margin (as opposed to gradually vanishing in the wing membrane before reaching the margin), and the presence of branches in the hind-wing RA.

Artimantodea is characterized by a relatively wide area between the anterior wing margin and ScP in the fore-wing, the MA fused to RA + RP in the fore-wing, and the complete absence of a median flexion line in the fore-wing. Within Artimantodea, the thespid *Miobantia fuscata* Giglio-Tos was recovered as sister to a group (node 7 in Fig. 6A, equivalent to Cernomantodea) defined by a large extension of the plicatum in the fore-wing (Fig. 6B-vi), and the presence of a cyclopean ear in the metathorax.

Assessment of tree sensitivity. The consistency index of individual characters is often considered a reliable metric for assessing phylogenetic tree robustness (Kluge & Farris, 1969). Of the 12 wing characters newly coded for this analysis, nine had an individual consistency index (c_i) of 1 in the strict consensus tree presented on Fig. 6 and in the Jackknife 50% majority-rule

Fig. 5. Details of plicatum and AA2* in hind-wing of stem- and crown-mantodeans. (A–E) Views encompassing the whole course of ppa; (A, B; and see E, F) *Labradormantis guilbaulti* **gen. et sp.n.**, paratype (MPEP702.11b), right hind-wing (negative imprint); (A) photograph (light-mirrored; RTI file extracts, see Appendix 1.4); (B) interpretative line drawing. (C) *Metallyticus splendidus* Westwood (IWC OB 194), plicatum in folded state, selection of vannal folds indicated, photograph; (D) *Chaeteessa filata* Burmeister (OUMNH-4566), plicatum in unfolded state (and see G), photograph; (E) interpretative line drawing as in B but with plicatum in unfolded state (as in D). (F, G) Close details of the position of ppa with respect to AA2*, as located in A and D, respectively; (F) photograph (light-mirrored; RTI file extracts, see Appendix 1.4); (G) photograph. Abbreviations and colour-coding: AA1, first anterior analis; AA2, second anterior analis; AA2*, first vein of second anterior analis; CuA, anterior cubitus; CuP, posterior cubitus; M, media; ppa, plica prima anterior (orange, dashed line); vf, vannal fold.

consensus tree (e.g. the AA2* hind-wing vein, the shape and location of the 'stigma', see Appendix 2.1). Furthermore, four of these had a c_i of 1 in the Bootstrap 50% majority-rule consensus tree as well (e.g. presence of a 'stigma', extension of the plicatum, see Appendix 2.1), indicating a strong fit on the tree. Consequently, the fact that major clades are supported by non-homoplastic character states demonstrates relatively high confidence in this strict consensus tree. Moreover, no ambiguous characters have been detected since all apomorphies in the obtained cladogram occurred under both ACCTRAN and DELTRAN optimizations.

Bremer support was also calculated to further assess tree sensitivity. It must be stressed that Mantodea, as well as the (*Chaeteessa* + sister group), (*Mantoida* + sister group) and (Metallyticidae + sister group) clades, required 2 additional steps to be collapsed (Appendix 2.3: Fig. S1A), thus key phylogenetic relationships were relatively well supported considering the amount of characters in the matrix. Artimantodea is the only clade with a Bremer support exceeding 2. Other consensus trees were produced using indirect measures of support. Jackknife support with 5% deletion was applied to a strict consensus tree in which only Artimantodea formed a consistently resolved clade (184 steps, CI = 0.380, RI = 0.305). It was also applied to a 50% majority-rule consensus tree in which a more resolved topology was recovered: outside Blattodea, the same clades as in the unsupported strict consensus tree were recovered in at least 91% of all replicates (105 steps, CI = 0.667, RI = 0.787, Appendix 2.3: Fig. S1B). The topology of the tree was not altered by a Jackknife test with 10% deletion, although some clades had slightly lesser support. Bootstrap support was applied to a strict consensus tree that recovered a completely unresolved polytomy (234 steps, CI = 0.299, RI = 0.000). It was also applied to a 50% majority-rule consensus tree that recovered polytomies between *Santanmantis*, *Labradormantis* **gen.n.** and *Baissomantis*, as well as between the MCM taxa (119 steps, CI = 0.588, RI = 0.701, Appendix 2.3: Fig. S1C).

Additionally, in order to further understand the results of these indirect measures of support, successive branch-and-bound searches were run, each excluding a different character from the matrix. The successive exclusion of apparently decisive characters (presence/absence of the stigma, AA2* and raptorial forelegs) was found not to affect tree topology at all, which confirms that several characters support the obtained relationships between the MCM taxa. However, the exclusion of the fore-wing ScP length (char. 5) from the matrix led to a polytomy between Blattodea and stem-mantodean taxa, suggesting that this character was essential to the recovery of a monophyletic Blattodea in this dataset. The exclusion of the stigma shape and location (char. 12) led to a polytomy between all stem-mantodeans, opening the possibility of a reversion to an ancestral state for *Santanmantis*. The lower stability of the Bootstrap results (relative to the Jackknife) is likely due to the added factor of randomly resampling characters (Siddall, 2002). The influence of *L. guilbaulti* **gen. et sp.n.** on tree topology was also tested by excluding it from the matrix. The resulting tree indicates the exact same relationships as the original (but see Discussion). This suggests

that taxon selection and character coding had a higher impact on the result.

Discussion

A unique combination of key characters in a new stem-mantodean

Considering that the fossil material of *Labradormantis guilbaulti* **gen. et sp.n.** mostly consists of fore-and hind-wings and that data of similar quality is lacking for the legs, head or abdomen, the matrix used in this contribution contained a higher proportion of wing characters than in previous morphology-based phylogenies (Grimaldi, 2003; Klass & Meier, 2006; Wieland, 2013; Delclòs *et al.*, 2016; Schwarz & Roy, 2019). The remarkable association of fore- and hind-wing data for the new species contributed to addressing phylogenetic relationships among fossil and extant mantodeans.

One of the key features is the occurrence (or lack thereof) of the fore-wing stigma, as well as its shape and location. Initial comparison of the wing venation of *L. guilbaulti* **gen. et sp.n.** and *Baissomantis picta* revealed many similarities. However, the apparent absence of a stigma in any *Baissomantis* specimen as documented in the literature raised doubts about the affinities of the two species, and on the placement of the latter within Dictyoptera. Our observations based on photographs of *Ba. picta* fore-wings revealed the occurrence of an oblique reddish-brown patch far more linear in shape than the surrounding spots, which we interpreted as the stigma (Fig. 4C). This input significantly changed the outcome of our preliminary phylogenetic analyses, with *Ba. picta* now firmly nested within Mantodea, as the sister taxon of *L. guilbaulti* **gen. et sp.n.**

The other key aspect regards the presence (or lack thereof) of a vein-like structure lying along the plica prima anterior (ppa) of the hind-wing. Smart (1956) first noticed this structure in *Chaeteessa*, which he identified as a genuine vein among a vannal system ('1V' in Smart 1956: Fig. 1). Since he had already noticed '1V' in the cockroach *Periplaneta americana* Linnaeus (Smart, 1951), he regarded the occurrence of this vein as a plesiomorphy within Dictyoptera. The hypothesis that '1V' is a genuine vein was contested on the grounds that its sclerotization appears less regular than that of surrounding veins, that it never forms a complete tube similar to other veins, and that its origin from AA2 is very faint. It was instead proposed that this structure was an intercalary between AA1 (another simple vein) and AA2 (which generally has posteriorly pectinate anterior branches), termed Iaa_1-aa_2 and that its unique presence in *Chaeteessa* was a derived trait (Brannoch *et al.*, 2017).

The hind-wing preservation of *L. guilbaulti* **gen. et sp.n.** offers a solution to this debate. The plicatum is folded underneath the remigium, with AA1, ppa and AA2 clearly visible (Fig. 5A, B). Only the anterior area of the plicatum is preserved, and it does not show any evidence of vannal folds. This configuration is similar to that of *Metallyticus*, where such folds are only
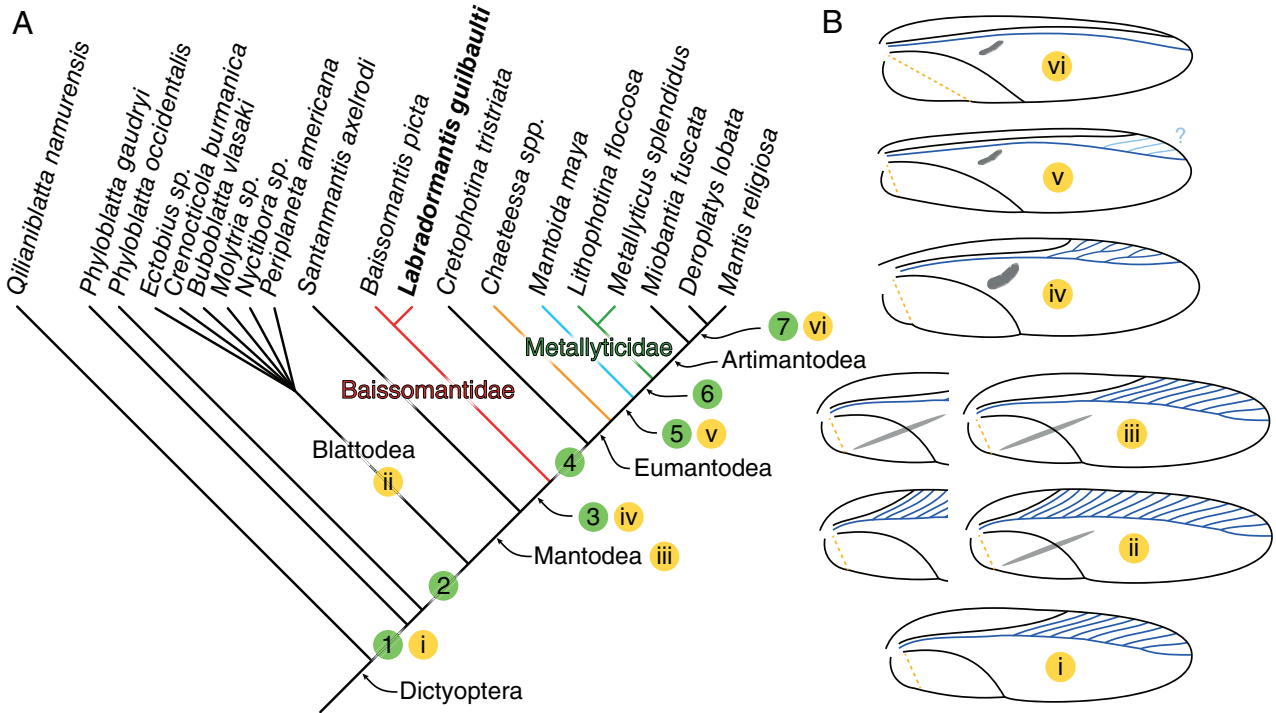
Fig. 6. Phylogenetic hypothesis and fore-wing morphological evolution of stem- and crown-Mantodea accounting for the character state combination displayed by *Labradormantis guilbaulti* **gen. et sp.n.** (A) Strict consensus tree of 60 equally parsimonious trees inferred from 61 morphological characters under equal weighting (105 steps, CI = 0.667, RI = 0.787). (B) Schematic drawings highlighting major steps in evolution of fore-wing stigma (grey), plicatum (orange, dashed line) and RA + RP branching pattern (blue) at certain nodes of the strict consensus tree, and relevant character states. Key wing characters at labelled nodes are as follows: **Node 1 (wing i)**: fore-wing RA + RP anteriorly pectinate, without well-differentiated RA and RP; **Node 2**: presence of stigma as line crossing CuP; **Blattodea (wings ii)**: ScP ending in basal quarter of fore-wing, stigma present on only one wing; **Mantodea (wings iii)**: stigma present on both fore-wings; **Node 3 (wing iv)**: stigma forming a patch restricted to the remigium; **Node 4**: ScP ending beyond apical third of fore-wing; **Node 5 (wing v)**: RA + RP (probably) simple along entire fore-wing, absence of AA2* in hind-wing; **Node 6**: fore-wing CuP with sigmoid curve, ScP ending beyond apical third of hind-wing; **Node 7 (wing vi)**: large extent of plicatum in fore-wing. [Colour figure can be viewed at wileyonlinelibrary.com].

occurring in the posterior area of the plicatum (Fig. 5C). The new fossil species displays a linear structure ('AA2*', the anteriormost vein of the second anterior analis, see Fig. 5E, F) almost as thick as AA1: it runs subparallel to the ppa, anterior to it basally, then superimposed onto it apically. This configuration was also observed in the specimen of *Chaeteessa filata* Burmeister studied by Smart (Fig. 5D, G). Basally, '1V'/AA2* is located anteriorly with respect to ppa, then superimposed onto it (and possibly posteriorly) apically. The fact that it is strongly sclerotized in the newly described fossil suggests that (1) it is a genuine vein and that (2) it is fading in *Chaeteessa*. AA2* was also detected on all blattodean wings included in our phylogenetic analysis (occurrence uncertain in *Crenocticola burmensis* Li & Huang; see original description). In well-preserved specimens of *Phyloblatta gaudryi* (see Béthoux *et al.*, 2011: Fig. 3), veins anterior to the ppa can be regarded as belonging to AA1, and the vein immediately posterior to them (emerging in the plicatum and crossing the ppa) can then be regarded as AA2*.

The detection of AA2* in a Cretaceous stem-mantodean thus supports Smart (1956)'s hypothesis according to which the ppa is associated with a simple vein ('1V'/AA2*) closely parallel

to it, and distinct from AA1 and from the rest of AA2 in Blattodea and *Chaeteessa*. Therefore, the lack of this vein was considered a secondary loss. It must be noted that we failed to corroborate the occurrence of AA2* in *Metallyticus* spp., as stated by Smart (1956). Nonetheless, based on our examination of photographs of a *Cretophotina tristriata* hind-wing (PIN 1989/2488), we corroborate the reconstruction provided by Gratshev & Zherikhin (1993: Fig. 1C), in which AA2* is represented.

L. guilbaulti **gen. et sp.n.** shares with *Creto. tristriata* a stigma restricted to the remigium and the occurrence of a well-developed AA2*. However, the new species also possesses a comparatively short fore-wing ScP, a plesiomorphy absent in *Creto. tristriata*. This combination therefore indicates that possessing a well-developed AA2* is ancestral to all mantodeans, its corollary being that lacking a well-developed AA2* is a state supporting a clade including *Mantoida*, *Metallyticus* and Artimantodea. These shared characters support *Chaeteessa* and its sister group as the most early-diverging extant mantodean lineage. This hypothesis was further tested by a formal cladistic analysis.

In summary, even though the inclusion of *L. guilbaulti* **gen. et sp.n.** was not directly responsible for the high resolution of our cladogram, it spurred a new hypothesis of homology for AA2* in Dictyoptera as a whole, which clearly enforced *Chaeteessa* as sister group of the remaining crown-mantodeans. This case is reminiscent of the discovery of the Pennsylvanian geropterans, which allowed the tracing of homologies of wing venation in Odonata with respect to other insects (Riek & Kukalová-Peck, 1984). It remains a classic example of the importance of fossils for systematic entomology. The present contribution further emphasizes that the inclusion of wing characters and fossil taxa within a phylogenetic dataset can be a useful complement to other characters, and even be indispensable to obtaining a highly resolved topology.

Relationships among extant and fossil mantodeans

The parsimony analysis yielded a fully resolved and robust cladogram for Mantodea (Fig. 6) and addresses the matter of the MCM relationships, a longstanding controversy in the order's phylogenetic tree. The retrieved topology is supported by the inclusion of an insofar unique combination of fossils (see Appendix 3.2 for more details) with a relatively wide spatial, temporal and taxonomic span.

Chaeteessa and its sister group are unequivocally retrieved as earlier-diverging than other mantodean lineages owing to the retention of several plesiomorphies, including a fully developed median flexion line in the fore-wing and the presence of AA2* in the hind-wing. The (*Chaeteessa* + other eumantodeans) node is defined by non-homoplastic characters and is relatively well supported (see Results). Additionally, *Chaeteessa* has only two discoidal spines on its fore femur (char. 42) and retains spines on its meso- and metathoracic 'walking' legs (chars. 47, 48; Wieland, 2013: chars. 83, 84). *Mantoida* and its sister group are then recovered as more early-diverging lineages than *Metallyticus* and Artimantodea due to a relatively short hind-wing ScP (char. 19). The vast majority of the character states in our analysis that support the derived position of *Metallyticus* as sister to Artimantodea do not occur on the wings, e.g. the absence of a torus intercervicalis in the intercervical sclerites of the cervix (char. 29; Wieland, 2013: char. 24) and the single row of antero-ventral spines on the fore femur (char. 38; Wieland, 2013: char. 45). As noted previously, *Metallyticus* displays highly derived head and leg characters combined with wing venation and proportions closely resembling those of blattodeans (Smart, 1956; Wieland, 2008, 2013). The derived position of this taxon in our analysis implies reversals in several wing characters. Most notably, the branching of RA + RP in the fore-wing (char. 1) and of RA in the hind-wing (char. 18) contrast markedly with the highly simplified and derived venation observed in *Mantoida*.

The topology obtained for the MCM taxa is in agreement with a recently updated classification of Mantodea based on a total-evidence approach combined with new data on genital anatomy (Schwarz & Roy, 2019). It also concurs on the placement of *Chaeteessa* (but not on that of *Mantoida* and *Metallyticus*) with other morphology-based (Wieland, 2013) and molecular-based phylogenies (Svenson & Whiting, 2009) (Fig. 1). Our analysis has recovered taxa equivalent to the Spinomantodea and Schizomantodea introduced in the most recent classification (Schwarz & Roy, 2019, pp. 122, 123). The corollary is that it supports *Chaeteessa* as sister to Spinomantodea (consisting in *Mantoida* + sister group) on the basis of the retention of spines on its walking legs. In contrast, the recovery of *Mantoida* as sister to Schizomantodea (consisting in Metallyticidae + Artimantodea) was achieved independently by both studies with completely different morphological characters. For instance, Schwarz & Roy (2019: p. 123) found a number of synapomorphies common to *Metallyticus* and artimantodean genitalia, most notably a secondary distal process on the ventral phallomere.

In our analysis, the branching order between *Mantoida* and *Metallyticus* was largely caused by the short hind-wing ScP in the former (a plesiomorphy). This result is opposed to Wieland (2013: p. 202), in which a long hind-wing ScP was scored for *Mantoida*, erroneously as it occurs. This discrepancy, along with the detection of a shared discoidal spine length pattern with more derived mantises, likely contributed to the recovery of *Mantoida* (instead of *Metallyticus*) as sister to Artimantodea by this author. As pointed out by Rivera & Svenson (2016: Fig. 4), the placement of *Metallyticus* remained contentious. Among other attempts, the maximum likelihood analysis obtained by Svenson & Whiting (2009: Figs 3, 5) yielded low nodal support values for the placement of this genus, either as sister to Artimantodea or nested within this group (Fig. 1C).

Although the relationships between the MCM taxa recovered in our parsimony analysis largely agree with the aforementioned studies, they are in disagreement with others for varying reasons. Previous phylogenies resting mainly on phallomere characters systematically recovered *Mantoida* and its sister group as the most early-diverging extant lineages (Klass, 1997; Klass & Meier, 2006). In contrast, our attempt, which combined phallomere characters together with wing and other body characters and included a broad selection of fossil taxa, retrieved *Chaeteessa* and its sister group as the most early-diverging mantodean lineages. However, it should be emphasized that phallomere-based changes in character state could not be traced due to a lack of documentation for stem-dictyopterans and stem-mantodeans included in the analysis coupled with unresolved relationships within Blattodea. As a consequence, phallomere-based characters could not be adequately polarized before node 4 (as in Fig. 6), i.e. after the position of *Chaeteessa* has been driven by other characters. As for other conflicting phylogenies, Legendre *et al.* (2015) not only recovered *Chaeteessa* deeply nested within Mantodea, but also mantoidids and metallyticids forming a clade sister to a fraction of Thespidae (i.e. not representing one of the earliest-diverging lineages; Fig. 1E). Such relationships were not recovered by any other investigations.

Besides the respective positions of the MCM taxa, the other controversy addressed by our analysis consists in the phylogenetic relationships among Cretaceous stem-mantodeans, which

remained poorly constrained. Attempts by Grimaldi (2003) and Delclòs *et al.* (2016) recovered largely unresolved topologies. These analyses also lacked a large selection of non-mantodean taxa to act as outgroups and assumed that *Baissomantis* belonged to a lineage that diverged earlier than *Santanmantis axelrodi*. In contrast, the latter was recovered as the earliest-diverging mantodean (along with its sister group) in the present contribution. This is largely due to new data on the fore-wing stigma in Baissomantidae (including the new fossil) and to a fuller polarization of its states achieved with the inclusion of blattodean and stem-dictyopteran representatives. It must also be emphasized that our ingroup selection, unlike that of Grimaldi (2003) and Delclòs *et al.* (2016), largely excluded fossils likely to act as rogue taxa due to a high proportion of missing character scores.

In this context, the close relationship between *Lithophotina floccosa* and *Metallyticus splendidus* Westwood is an unexpected result. This is the first phylogenetic analysis to include this extinct eumantodean, discovered in the late Eocene Florissant locality (Colorado, U.S.A.). It had previously been assigned to Chaeteessidae following the description by Sharov (1962) of a hind-wing discovered in 1953 at the same locality as the fore-wing holotype. This systematic placement was based on 'the different character of the venation of the fore and hind-wings, and also the ratio of the length of the fore and hind-wing of *L. floccosa*, […] very close to that of *Chaeteessa filata* Burm.' (Sharov, 1962: p. 103), which equally applies to Metallyticidae. It must be acknowledged, however, that by 1962 the wing venation of metallyticids was poorly documented (see Wieland, 2008; and references therein), as opposed to that of *Chaeteessa*, documented by Smart (1956) a few years earlier. Our result suggests a very close relationship between *Lithophotina* and *Metallyticus* on the basis of several character states, including a long ScP in the hind-wing (char. 19), a sigmoid CuP in the fore-wing (char. 2, both shared between metallyticids and some artimantodeans), and a branched RA + RP in the hind-wing, the latter being a reversal according to our analysis. The late branching of CuA in the hind-wing distinguishes it from crown-Metallyticidae. In light of this result, closer investigations may be needed to assess more thoroughly the possible affinities of *Lithophotina* to Metallyticidae.

Patterns of mantodean wing evolution

This study clarifies the sequence of character state acquisition underlying the evolution of mantis morphology (Fig. 6B). Soon after the acquisition of raptorial forelegs, which took place along the stem leading to *Santanmantis* and other mantodeans, several modifications affected the fore-wing stigma. In turn, Baissomantidae is excluded from the group including *Cretophotina* and Eumantodea because of the retention of a plesiomorphic, medium-sized ScP in the fore-wing. In contrast, the reduction of the median flexion line, the gradual loss of AA2* in the hind-wing, and the complete simplification of the fore-wing RA + RP occurred

among lineages resulting from the earliest splitting events within Eumantodea (including the MCM taxa). Ultimately, the expanded fore-wing plicatum was acquired within Artimantodea.

This clearer phylogenetic framework may serve as a foundation for addressing evolutionary aspects of wing biomechanics in Mantodea. While dictyopterans retain fully developed fore- and hind-wings, they are infrequent flyers, with a more cursorial lifestyle in comparison with other polyneopterans (Grimaldi & Engel, 2005; Djernæs, 2018; Wieland & Svenson, 2018). Typically, their fore-wings are more strongly sclerotized, possibly as a means of protecting the hind-wings when at rest. Similarly, early-diverging lineages such as *Baissomantis* and *Santanmantis* tend to possess moderately to well-sclerotized fore-wings (see Gratshev & Zherikhin, 1993; Grimaldi, 2003; Hörnig *et al.*, 2017), indicative of a more concealed and cursorial lifestyle on bark and leaf litter. As for the hind-wing, the scarce available documentation on the flight of praying mantises (Brackenbury, 1990, 1991) suggests that this structure has a prominent role in generating lift.

The application of the theory of evolutionary modularity and integration (Schlosser & Wagner, 2004; Klingenberg, 2008) to mantodean and blattodean wing venation could offer additional clues on their relatively poor flight performances. The only study to apply them to insect wings at a macro-evolutionary scale detected a very high degree of integration between venational elements across 189 dragonfly species (Blanke, 2018), which may have been key to the evolution of advanced flight performance in Odonatoptera (Azuma & Watanabe, 1988; Bybee *et al.*, 2008; Jongerius & Lentink, 2010). This idea could be developed further by testing for similar patterns in less frequent flyers, such as dictyopterans.

The fore-wing of mantodeans, for instance, is hypothesized to have evolved increased modularity. In the most plesiomorphic mantodean wings, the stigma spanned the clavus and the remigium (e.g. *Santanmantis*; Fig. 6B-iii), which implies a wing with relatively low regional specialization. Once the stigma was reduced to a patch on the remigium (as in baissomantids such as *Labradormantis guilbaulti* **gen. et sp.n.**; Fig. 6B-iv), the clavus and remigium might have become relatively decoupled, thus forming two functional modules. The trajectory of ScP and RA + RP as simple elongated veins parallel and close to the wing margin could have led to a third module by further dividing the remigium (Fig. 6B-v). Eventually, in artimantodeans, the enlarged fore-wing plicatum (Fig. 6B-vi) could be considered as a complement to the 'clavus module', with which it forms a single cambered area during downstroke (Brackenbury, 1991: pl. V). This particular configuration likely augmented the lift generated by the fore-wing.

In contrast, the hind-wing is hypothesized to have evolved towards an ever more integrated structure, in relation to the progressive loss of the AA2*. In cockroaches, this vein appears to delimit two functional modules: a rigid remigium acting as a leading element, and a flexible plicatum acting as a trailing element generating most of the lift during downstroke. Under this hypothesis, AA2* in particular would form a rod

guiding the movements of the plicatum. Its partial degradation in *Chaeteessa* and complete loss in all other extant mantises (node 5 on Fig. 6B) could be related to the merging of both the remigium and plicatum into a single functional unit. Indeed, artimantodeans possess very flexible hind-wing remigia (Brackenbury, 1991), i.e. more capable of generating lift. This change in flight performance may have played a role in predator avoidance, concurrently to the development of dedicated sensory structures such as the cyclopean ear (Yager & Svenson, 2008).

These trends are indicative of a comparatively specialized flight behaviour for modern mantises relative to insects that possess fore- and hind-wings sharing a more similar function. They also suggest that artimantodean flight may indeed be uniquely derived from relatives with seemingly lesser flight abilities. Our phylogenetic analysis positions *Chaeteessa* as a particularly promising study system to test the latter hypothesis. However, our current knowledge of the life history of the five known chaeteessid species (Wieland & Svenson, 2018) is highly deficient: it is limited to scarce observations in Neotropical rainforests suggesting that they are bark-dwelling mantises with a lifestyle similar to that of *Metallyticus* (Salazar, 2004, 2005; Wieland, 2008; Bustamante-Navarrete, 2018). In conclusion, a more exhaustive documentation of flying mantises and cockroaches is required to better understand the relationship between wing morphology and flight performance across the phylogenetic system of Dictyoptera.

Conclusion

For several insect taxa, the bulk of extant diversity is composed of groups that diversified relatively recently, during the Cretaceous or later (Evangelista, et al., 2019b; Simon *et al.*, 2019), the corollary being that the diversity of their respective sister groups remained low. Moreover, the latter often display peculiar morphologies and/or ecological preferences, which can render phylogenetic investigations challenging. This is the case, for instance, of *Timema* Scudder, the sister group of all other crown-Phasmatodea (Bradler, 1999, 2009; Whiting *et al.*, 2003). In contrast to other stick-insects, it is apterous in both sexes, has fewer than five tarsal segments, and inhabits gymnosperms (Kristensen, 1975; Vickery, 1993; Tilgner *et al.*, 1999). The same pattern applies to Mantodea, with the species-poor MCM taxa displaying highly disparate morphologies, introducing uncertainties on the early evolution of this group.

The discovery of the baissomantid *Labradormantis guilbaulti* **gen. et sp.n.** led to a reconsideration of wing characters that proved to have a decisive influence on this phylogenetic jigsaw. Its unique combination of ancestral and derived states, complemented by new characters and an extensive taxon selection, situated Baissomantidae as transitional forms within Mantodea. On one hand, baissomantids retain a fore-wing ScP of medium length, as well as an AA2* vein running along the folding line of the hind-wing. On the other, they

are, together with their sister group, the earliest-diverging mantodeans

It is hoped that the present contribution, based on an updated dataset, will prompt a renewed interest in wing morphology for phylogenetic investigations on insects. Beyond topographic homologies, fossil wings hold a particular advantage since they can be scored on very ancient plesiotypic lineages, which enables the polarization of otherwise ambiguous characters. Furthermore, this study has demonstrated the extent to which wings can impact insect phylogenies among other morphological characters by revealing transitional phenotypes preceding modern derived clades, as well as the insight they can offer on the biology of extinct insect taxa.

Supporting Information

Additional supporting information may be found online in the Supporting Information section at the end of the article.

Appendix S1: RTI files of the type specimens of *Labradormantis guilbaulti* **gen. et sp.n.**

Appendix 1.1: holotype MPEP1157.6, complete specimen view.

Appendix 1.2: paratype MPEP702.11, complete view of part (MPEP702.11a).

Appendix 1.3: paratype MPEP702.11, complete view of counterpart (MPEP702.11b).

Appendix 1.4: paratype MPEP702.11b, closeup of plicatum. Instructions for downloading the RTI files are provided in a .rtf file.

Appendix S2: Supplementary files for phylogenetic analysis.

Appendix 2.1 provides coding, references and consistency, retention and homoplasy indices for the characters used to form the character matrix.

Appendix 2.2 presents the character matrix in nexus format.

Appendix 2.3: **Fig. S1** presents the main results of various measures of branch support to assess the sensitivity of our strict consensus tree to the parsimony analysis.

Appendix S3: Supplementary text.

Appendix 3.1 is an extended description of the type specimens of *Labradormantis guilbaulti* **gen. et sp.n.** with added information on characters which were not relevant to the parsimony analysis and a discussion on the assignment of both fossil specimens to the same species.

Appendix 3.2 discusses the role of fossil and extant taxa selected in the phylogenetic dataset to polarize certain morphological characters and thus resolve our strict consensus tree.

Acknowledgements

Data availability statement

The data that support the findings of this study are available in the Open Science Framework (Demers-Potvin et al., 2020a).

References

Agnarsson, I. & Miller, J.A. (2008) Is ACCTRAN better than DEL-TRAN? *Cladistics*, **24**, 1032–1038. https://doi.org/10.1111/j.1096-0031.2008.00229.x.

Agnus, A.N. (1903) Deuxième note sur les Blattidae paléozoïques (Orthopt. Palaeoz.). Description d'une espèce nouvelle. *Bulletin de La Société Entomologique de France*, **17**, 291–294.

Agudelo, A.A. (2014) A new genus and species of Mantoididae (Mantodea) from the Brazilian and Venezuelan Amazon, with remarks on *Mantoida* Newman, 1838. *Zootaxa*, **3797**, 194–206. https://doi.org/10.11646/zootaxa.3797.1.14.

Azuma, A. & Watanabe, T. (1988) Flight performance of a dragonfly. *Journal of Experimental Biology*, **137**, 221–252.

Bai, M., Beutel, R.G., Klass, K.-D., Zhang, W., Yang, X. & Wipfler, B. (2016) †Alienoptera – a new insect order in the roach–mantodean twilight zone. *Gondwana Research*, **39**, 317–326. https://doi.org/10.1016/j.gr.2016.02.002.

Belahmira, A., Schneider, J.W., Scholze, F. & Saber, H. (2019) Phyloblattidae and Compsoblattidae (Insecta, Blattodea) from the late Carboniferous Souss basin, Morocco. *Journal of Paleontology*, **93**, 945–965. https://doi.org/10.1017/jpa.2019.20.

Béthoux, O. (2005) Wing venation pattern of Plecoptera (Insecta: Neoptera). *Illiesia*, **1**, 52–81.

Béthoux, O. & Wieland, F. (2009) Evidence for Carboniferous origin of the order Mantodea (Insecta: Dictyoptera) gained from forewing morphology. *Zoological Journal of the Linnean Society*, **156**, 79–113. https://doi.org/10.1111/j.1096-3642.2008.00485.x.

Béthoux, O., Schneider, J.W. & Klass, K.-D. (2011) Redescription of the holotype of *Phyloblatta gaudryi* (Agnus, 1903) (Pennsylvanian; Commentry, France), an exceptionally well-preserved stem-dictyopteran. *Geodiversitas*, **33**, 625–635. https://doi.org/10.5252/g2011n4a4.

Béthoux, O., Llamosi, A. & Toussaint, S. (2016) Reinvestigation of *Protelytron permianum* (Insecta; early Permian; USA) as an example for applying reflectance transformation imaging to insect imprint fossils. *Fossil Record*, **20**, 1–7. https://doi.org/10.5194/fr-20-1-2016.

Blais, R.A. (1959) L'origine des minerais crétacés du gisement de fer de Redmond, Labrador. *Le Naturaliste Canadien*, **86**, 265–299.

Blanke, A. (2018) Analysis of modularity and integration suggests evolution of dragonfly wing venation mainly in response to functional demands. *Journal of the Royal Society Interface*, **15**, 20180277. https://doi.org/10.1098/rsif.2018.0277.

Brackenbury, J. (1990) Wing movements in the bush-cricket *Tettigonia viridissima* and the mantis *Ameles spallanziana* during natural leaping. *Journal of Zoology*, **220**, 593–602. https://doi.org/10.1111/j.1469-7998.1990.tb04737.x.

Brackenbury, J. (1991) Wing kinematics during natural leaping in the mantids *Mantis religiosa* and *Iris oratoria*. *Journal of Zoology*, **223**, 341–356. https://doi.org/10.1111/j.1469-7998.1991.tb04769.x.

Bradler, S. (1999) The vomer of *Timema* Scudder, 1895 (Insecta: Phasmatodea) and its significance for phasmatodean phylogeny. *Courier Forschungsinstitut Senckenberg*, **215**, 43–47.

Bradler, S. (2009) Die Phylogenie der Stab- und Gespenstschrecken (Insecta: Phasmatodea). *Species, Phylogeny and Evolution*, **2**, 3–139. https://doi.org/10.17875/gup2009-710.

Brannoch, S.K., Wieland, F., Rivera, J., Klass, K.-D., Béthoux, O. & Svenson, G.J. (2017) Manual of praying mantis morphology, nomenclature, and practices (Insecta, Mantodea). *ZooKeys*, **696**, 1–100. https://doi.org/10.3897/zookeys.696.12542.

Burmeister, H.C. (1838) Fangschrecken, Mantodea. *Handbuch der Entomologie: Vol. 2: v-viii (pp. 517–522)* (ed. by T.C.F. Enslin). Berlin: Theodor Christian Friedrich Enslin.

Bustamante-Navarrete, A. (2018) First record of *Chaeteessa nigromarginata* from Peru (Mantodea: Chaeteessidae). *Fragmenta Entomologica*, **50**, 171–174.

Bybee, S.M., Ogden, T.H., Branham, M.A. & Whiting, M.F. (2008) Molecules, morphology and fossils: a comprehensive approach to odonate phylogeny and the evolution of the odonate wing. *Cladistics*, **24**, 477–514. https://doi.org/10.1111/j.1096-0031.2007.00191.x.

Carpenter, F.M. (1967) Cretaceous insects from Labrador 2. A new family of snake-flies (Neuroptera: Alloraphidiidae). *Psyche: A Journal of Entomology*, **74**, 270–275.

Cockerell, T. D. A. (1908) The first American fossil *Mantis*. *The Canadian Entomologist*, **40**, 343–344.

Cui, Y., Evangelista, D.A. & Béthoux, O. (2018) Prayers for fossil mantis unfulfilled: *Prochaeradodis enigmaticus* Piton, 1940 is a cockroach (Blattodea). *Geodiversitas*, **40**, 355–362. https://doi.org/10.5252/geodiversitas2018v40a15.

Delclòs, X., Peñalver, E., Arillo, A., Engel, M.S., Nel, A., Azar, D. & Ross, A. (2016) New mantises (Insecta: Mantodea) in Cretaceous

ambers from Lebanon, Spain, and Myanmar. *Cretaceous Research*, **60**, 91–108. https://doi.org/10.1016/j.cretres.2015.11.001.

Demers-Potvin, A.V. & Larsson, H.C.E. (2019) Palaeoclimatic reconstruction for a Cenomanian-aged angiosperm flora near Schefferville, Labrador. *Palaeontology*, **62**, 1027–1048. https://doi.org/10.1111/pala.12444.

Demers-Potvin, A.V., Larsson, H., Cournoyer, M. & Béthoux, O. (2020a) Data from: wing morphology of a new Cretaceous praying mantis solves the phylogenetic jigsaw of early-diverging extant lineages. *OSF*. https://doi.org/10.17605/OSF.IO/R8UF7.

Demers-Potvin, A.V., Szwedo, J., Paragnani, C. & Larsson, H.C.E. (2020b) First north American occurrence of hairy cicadas discovered in the Cenomanian (Late Cretaceous) of Labrador, Canada. *Acta Palaeontologica Polonica*, **65**, 85–98. https://doi.org/10.4202/app.00669.2019.

Dittmann, I.L., Hörnig, M.K., Haug, J.T. & Haug, C. (2015) *Raptoblatta waddingtonae* n. gen. et n. sp. – an Early Cretaceous roach-like insect with a mantodean-type raptorial foreleg. *Palaeodiversity*, **8**, 103–111.

Djernæs, M. (2018) Biodiversity of Blattodea – the cockroaches and termites. *Insect Biodiversity: Science and Society* (ed. by R.G. Foottit and P.H. Adler), pp. 359–387. Hoboken: Wiley-Blackwell. https://doi.org/10.1002/9781118945582.ch14.

Dorf, E. (1959) Cretaceous flora from beds associated with rubble iron-ore deposits in the Labrador trough. *Bulletin of the Geological Society of America*, **70**, 1591.

Dorf, E. (1967) Cretaceous insects from Labrador I. geologic occurrence. *Psyche: A Journal of Entomology*, **74**, 267–269.

Ehrmann, R. (2002) *Mantodea: Gottesanbeterinnen der Welt*. Münster: Natur und Tier-Verlag.

Emerson, A.E. (1967) Cretaceous insects from Labrador 3. A new genus and species of termite. (Isoptera: Hodotermitidae). *Psyche: A Journal of Entomology*, **74**, 276–289.

Evangelista, D.A., Kotyková Varadínová, Z., Jůna, F., Grandcolas, P. & Legendre, F. (2019a) New cockroaches (Dictyoptera: Blattodea) from French Guiana and a revised checklist for the region. *Neotropical Entomology*, **48**, 645–659. https://doi.org/10.1007/s13744-019-00677-6.

Evangelista, D.A., Wipfler, B., Béthoux, O. *et al.* (2019b) An integrative phylogenomic approach illuminates the evolutionary history of cockroaches and termites (Blattodea). *Proceedings of the Royal Society B: Biological Sciences*, **286**, 20182076. https://doi.org/10.1098/rspb.2018.2076.

Giglio-Tos, E. (1917) Mantidi Esotici Generi e Specie Nuove. *Bulletino Della Società Entomologica Italiana*, **48**, 43–108.

Gratshev, V.G. & Zherikhin, V.V. (1993) New fossil mantids (Insecta, Mantida [sic]). *Paleontological Journal*, **27**(1A), 148–165.

Grimaldi, D.A. (2003) A revision of Cretaceous mantises and their relationships, including new taxa (Insecta: Dictyoptera: Mantodea). *American Museum Novitates*, **3412**, 1–47. https://doi.org/10.1206/0003-0082(2003)412<0001:AROCMA>2.0.CO;2.

Grimaldi, D.A. & Engel, M.S. (2005) *Evolution of the Insects*. New York: Cambridge University Press.

Guérin-Méneville, F.E. (1838) Première division. Insectes, Arachnides et Crustacés. In: L. I. Duperrey (Ed.), *Voyage autour du monde, exécuté par ordre du Roi, sur la corvette de sa Majesté, La Coquille, pendant les années 1822, 1823, 1824 et 1825. Zoologie* (pp. 1–319). Bertrand, H.

Guo, Y., Béthoux, O., Gu, J. & Ren, D. (2013) Wing venation homologies in Pennsylvanian 'cockroachoids' (Insecta) clarified thanks to a remarkable specimen from the Pennsylvanian of Ningxia (China). *Journal of Systematic Palaeontology*, **11**, 41–46. https://doi.org/10.1080/14772019.2011.637519.

Hörnig, M.K., Haug, J.T. & Haug, C. (2013) New details of *Santanmantis axelrodi* and the evolution of the mantodean morphotype. *Palaeodiversity*, **6**, 157–168.

Hörnig, M.K., Haug, J.T. & Haug, C. (2017) An exceptionally preserved 110 million years old praying mantis provides new insights into the predatory behaviour of early mantodeans. *PeerJ*, **5**, e3605. https://doi.org/10.7717/peerj.3605.

Jongerius, S.R. & Lentink, D. (2010) Structural analysis of a dragonfly wing. *Experimental Mechanics*, **50**, 1323–1334. https://doi.org/10.1007/s11340-010-9411-x.

Klass, K.-D. (1997) *The external male genitalia and phylogeny of Blattaria and Mantodea* (Bonner Zoologische Monographien, Vol. 42). *Zoologisches Forschungsinstitut*. Bonn: Zoologisches Forschungsinstitut.

Klass, K.-D. & Meier, R. (2006) A phylogenetic analysis of Dictyoptera (Insecta) based on morphological characters. *Entomologische Abhandlungen*, **63**, 3–50.

Klingenberg, C.P. (2008) Morphological integration and developmental modularity. *Annual Review of Ecology, Evolution, and Systematics*, **39**, 115–132. https://doi.org/10.1146/annurev.ecolsys.37.091305.110054.

Kluge, A.G. & Farris, J.S. (1969) Quantitative Phyletics and the evolution of anurans. *Systematic Zoology*, **18**, 1–32.

Kočárek, P. (2019) *Alienopterella stigmatica* gen. et sp. nov.: the second known species and specimen of Alienoptera extends knowledge about this Cretaceous order (Insecta: Polyneoptera). *Journal of Systematic Palaeontology*, **17**, 491–499. https://doi.org/10.1080/14772019.2018.1440440.

Kristensen, N.P. (1975) The phylogeny of hexapod "orders". A critical review of recent accounts. *Journal of Zoological Systematics and Evolutionary Research*, **13**, 1–44. https://doi.org/10.1111/j.1439-0469.1975.tb00226.x.

Kukalová-Peck, J. (1991) Fossil history and the evolution of hexapod structures. *The Insects of Australia*, 2nd edn, Vol. **1** (ed. by I.D. Naumann), pp. 141–179. Melbourne: Melbourne University Press.

Lameere, A. (1922) Sur la nervation alaire des insectes [on the wing venation of insects]. *Bulletin de la Classe des Sciences de l'Académie Royale de Belgique, Bruxelles*, **8**, 138–149.

Lameere, A. (1923) On the wing-venation of insects. *Psyche: A Journal of Entomology*, **30**, 123–132. https://doi.org/10.1155/1923/16920.

Laurentiaux-Vieira, F. & Laurentiaux, V. (1980) Nouvelle contribution à la connaissance du genre Westphalien *Manoblatta* Pruvost (Blattaires, Archymylacridiens). *Annales de La Société Géologique Du Nord*, **99**, 415–423.

Lee, S.-W. (2014) New Lower Cretaceous basal mantodean (Insecta) from the Crato formation (NE Brazil). *Geologica Carpathica*, **65**, 285–292. https://doi.org/10.2478/geoca-2014-0019.

Legendre, F., Nel, A., Svenson, G.J., Robillard, T., Pellens, R. & Grandcolas, P. (2015) Phylogeny of Dictyoptera: dating the origin of cockroaches, praying mantises and termites with molecular data and controlled fossil evidence. *PLoS One*, **10**, e0130127. https://doi.org/10.1371/journal.pone.0130127.

Li, X.-R. & Huang, D. (2018) A new praying mantis from middle Cretaceous Burmese amber exhibits bilateral asymmetry of forefemoral spination (Insecta: Dictyoptera). *Cretaceous Research*, **91**, 269–273. https://doi.org/10.1016/j.cretres.2018.06.019.

Li, X.-R. & Huang, D. (2020) A new mid-Cretaceous cockroach of stem Nocticolidae and reestimating the age of Corydioidea (Dictyoptera: Blattodea). *Cretaceous Research*, **106**, 104202. https://doi.org/10.1016/j.cretres.2019.104202.

Linnaeus, C. (1758) Systema naturae per regna tria naturae, secundum classes, ordines, genera, species, cum characteribus, differentiis,

synonymis, locis: Vol. Tomus I (Tomus I. Editio decima, reformata). Laurentii Salvii.

Loxton, R.G. & Nicholls, I. (1979) The functional morphology of the praying mantis forelimb (Dictyoptera: Mantodea). *Zoological Journal of the Linnean Society*, **66**, 185–203. https://doi.org/10.1111/j.1096-3642.1979.tb01908.x.

Maddison, W.P., & Maddison, D.R. (2018) Mesquite: A modular system for evolutionary analysis. Version 3.61. http://www.mesquiteproject .org

Misof, B., Liu, S., Meusemann, K. *et al.* (2014) Phylogenomics resolves the timing and pattern of insect evolution. *Science*, **346**, 763–767.

Newman, E. (1838) Natural Order (nov. Gen. *Mantoida*). *Entomological Magazine*, **5**, 178–179.

Piton, L.E. (1940) Paléontologie du Gisement Éocène de Menat (Puy-de-Dôme) (flore et faune). *Mémoires de La Société d'Histoire Naturelle d'Auvergne*, **1**, 1–303.

Ponomarenko, A.G. (1969) Cretaceous insects from Labrador. 4. A new family of beetles (Coleoptera: Archostemata). *Psyche: A Journal of Entomology*, **76**, 306–310.

Pruvost, P. (1919) Introduction à l'étude du terrain houiller du Nord et du Pas-de-Calais. *La faune continentale du terrain houiller du Nord de la France*, **2**.1–584.

Ragge, D.R. (1955) *The Wing-Venation of the Orthoptera Saltatoria, with Notes on Dictyopteran Wing-Venation*. London: Trustees of the British Museum of Natural History.

Reflectance Transformation Imaging (RTI). (2019) Cultural Heritage Imaging: Helping Humanity Save History. http:// culturalheritageimaging.org/Technologies/RTI/

Rice, H.M.A. (1969) An antlion (Neuroptera) and a stonefly (Plecoptera) of Cretaceous age from Labrador, Newfoundland. *Geological Survey of Canada, Department of Energy, Mines and Resources, Paper*, **68–65**, iv + 1–iv + 11.

Riek, E.F. & Kukalová-Peck, J. (1984) A new interpretation of dragonfly wing venation based upon Early Upper Carboniferous fossils from Argentina (Insecta: Odonatoidea) and basic character states in pterygote wings. *Canadian Journal of Zoology*, **62**, 1150–1166. https://doi.org/10.1139/z84-166.

Rivera, J. & Callohuari, Y. (2019) A new species of praying mantis from Peru reveals impaling as a novel hunting strategy in Mantodea (Thespidae: Thespini). *Neotropical Entomology.*, **49**, 234–249. https://doi.org/10.1007/s13744-019-00744-y.

Rivera, J. & Svenson, G.J. (2016) The Neotropical 'polymorphic earless praying mantises' – part I: molecular phylogeny and revised higher-level systematics (Insecta: Mantodea, Acanthopoidea): phylogeny of polymorphic earless praying mantises. *Systematic Entomology*, **41**, 607–649. https://doi.org/10.1111/syen.12178.

Ross, A.J. (2012) Testing decreasing variability of cockroach forewings through time using four recent species: *Blattella germanica*, *Polyphaga aegyptiaca*, *Shelfordella lateralis* and *Blaberus craniifer*, with implications for the study of fossil cockroach forewings. *Insect Science*, **19**, 129–142. https://doi.org/10.1111/j.1744-7917.2011 .01465.x.

Salazar, J.A. (2004) Nuevas especies de blátidos y mántidos para Colombia (Insecta: Dictyoptera) y una nota sobre la hembra de *Vates festae* Giglio-Tos, 1914. *Boletín Científico Museo de História Natural*, **8**, 267–286.

Salazar, J.A. (2005) Notas sobre *Metallyticus* Westwood, 1837; *Chaeteessa* Burmeister, 1838 y *Mantoida* Newman, 1838. Tres géneros primitivos de mantidos tropicales (Dictyoptera: Mantodea). *Lambillionea*, **2**, 265–276.

de Saussure, H. & Zehntner, L. (1894) Biologia centrali-americana. Insecta. Orthoptera. Fam. Mantidae. *Société Entomologique Zurich*, **1**, 123–197.

Scherrer, M.V. (2014) A revision of *Miobantia* Giglio-Tos, 1917 (Mantodea: Thespidae, Miobantiinae), with molecular association of dimorphic sexes and immature stages. *Zootaxa*, **3797**, 207–268. https://doi.org/10.11646/zootaxa.3797.1.15.

Schindelin, J., Arganda-Carreras, I., Frise, E. *et al.* (2012) Fiji: an open-source platform for biological-image analysis. *Nature Methods*, **9**, 676–682. https://doi.org/10.1038/nmeth.2019.

Schlosser, G. & Wagner, G.P. (2004) *Modularity in Development and Evolution*. Chicago: University of Chicago Press.

Schneider, J.W. (1977a) Zur Variabilität der Flügel paläozoischer Blattodea (Insecta), Teil I. *Freiberger Forschungshefte, C*, **326**, 87–106.

Schneider, J.W. (1977b) Zur Variabilität der Flügel paläozoischer Blattodea (Insecta), Teil II. *Freiberger Forschungshefte, C*, **334**, 21–39.

Schneider, J.W. (1984) Die Blattodea (Insecta) des Paläozoikums. *Teil II: Morphogenese der Flügelstrukturen und Phylogenie. Freiberger Forschungshefte, C*, **391**, 5–34.

Schwarz, C.J. & Roy, R. (2019) The systematics of Mantodea revisited: an updated classification incorporating multiple data sources (Insecta: Dictyoptera). *Annales de La Société Entomologique de France (N.S.)*, **55**, 101–196. https://doi.org/10.1080/00379271.2018.1556567.

Scudder, S.H. (1890) New types of cockroaches from the Carboniferous deposits of the United States. *Memoirs of the Boston Society of Natural History*, **4**, 401–415.

Scudder, S.H. (1895) Summary of the U. S. Phasmids. *The Canadian Entomologist*, **27**, 29–30.

Sharov, A.G. (1962) Redescription of *Lithophotina floccosa* Cock. (Manteodea) with some notes on the manteod wing venation. *Psyche: A Journal of Entomology*, **69**, 102–106. https://doi.org/10.1155/1962/ 67682.

Siddall, M.E. (2002) Measures of support. *Techniques in Molecular Systematics and Evolution (pp. 80–101)* (ed. by R. DeSalle, G. Giribet and W. Wheeler). Birkhäuser, Basel. https://doi.org/10.1007/978-3-0348-8125-8_5.

Simon, S., Letsch, H., Bank, S *et al.* (2019) Old World and New World Phasmatodea: Phylogenomics resolve the evolutionary history of stick and leaf insects. *Frontiers in Ecology and Evolution*, **7**, 1–14. https:// doi.org/10.3389/fevo.2019.00345.

Smart, J. (1951) The wing-venation of the American cockroach *Periplaneta americana* Linn. (Insecta: Blattidae). *Proceedings of the Zoological Society of London*, **121**, 501–511.

Smart, J. (1956) On the wing-venation of *Chaeteessa* and other mantids (Insecta: Mantodea). *Proceedings of the Zoological Society of London*, **127**, 545–553. https://doi.org/10.1111/j.1096-3642.1956 .tb00487.x.

Svenson, G.J. & Rodrigues, H.M. (2019) A novel form of wasp mimicry in a new species of praying mantis from the Amazon rainforest, *Vespamantoida wherleyi* gen. nov. sp. nov. (Mantodea, Mantoididae). *PeerJ*, **7**, e7886. https://doi.org/10.7717/peerj.7886.

Svenson, G.J. & Whiting, M.F. (2004) Phylogeny of Mantodea based on molecular data: evolution of a charismatic predator. *Systematic Entomology*, **29**, 359–370. https://doi.org/10.1111/j.0307-6970.2004 .00240.x.

Svenson, G.J. & Whiting, M.F. (2009) Reconstructing the origins of praying mantises (Dictyoptera, Mantodea): the roles of Gondwanan vicariance and morphological convergence. *Cladistics*, **25**, 468–514. https://doi.org/10.1111/j.1096-0031.2009.00263.x.

Svenson, G.J., Hardy, N.B., Wightman, H.M.C. & Wieland, F. (2015) Of flowers and twigs: phylogenetic revision of the plant-mimicking praying mantises (Mantodea: Empusidae and Hymenopodidae) with a new suprageneric classification. *Systematic Entomology*, **40**, 789–834. https://doi.org/10.1111/syen.12134.

Svenson, G.J., Medellin, C. & Sarmiento, C.E. (2016) Re-evolution of a morphological precursor of crypsis investment in the newly revised horned praying mantises (Insecta, Mantodea, Vatinae). *Systematic Entomology*, **41**, 229–255. https://doi.org/10.1111/syen .12151.

Swofford, D.L. (2002) *PAUP* Version 4.0 b10. Phylogenetic Analysis Using Parsimony (* and Other Methods)*, Sunderland: Sinauer.

Tilgner, E.H., Kiselyoval, T.G. & McHugh, J.V. (1999) A morphological study of *Timema cristinae* Vickery with Implications for the Phylogenetics of Phasmida. *Deutsche Entomologische Zeitschrift*, **46**, 149–162.

Vickery, V.R. (1993) Revision of *Timema* Scudder (Phasmatoptera: Timematodea) including three new species. *The Canadian Entomologist*, **125**, 657–692. https://doi.org/10.4039/Ent125657-4.

Wei, D., Béthoux, O., Guo, Y., Schneider, J.W. & Ren, D. (2013) New data on the singularly rare 'cockroachoids' from Xiaheyan (Pennsylvanian; Ningxia, China). *Alcheringa*, **37**, 547–557. https:// doi.org/10.1080/03115518.2013.808863.

Westwood, J.O. (1835) Insectorum Arachnoidumque novorum decades duo. *Zoological Journal*, **5**, 440–443.

Whiting, M.F., Bradler, S. & Maxwell, T. (2003) Loss and recovery of wings in stick insects. *Nature*, **421**, 264–267. https://doi.org/10.1038/ nature01313.

Wieland, F. (2008) The genus *Metallyticus* reviewed (Insecta: Mantodea). *Species, Phylogeny and Evolution*, **1**, 147–170.

Wieland, F. (2013) The phylogenetic system of Mantodea (Insecta: Dictyoptera). *Species, Phylogeny and Evolution*, **3**, 3–222. https://doi .org/10.17875/gup2013-711.

Wieland, F. & Svenson, G.J. (2018) Biodiversity of Mantodea. *Insect Biodiversity: Science and Society*, Vol. **2** (ed. by R.G. Foottit and P.H. Adler), pp. 389–416. Hoboken: Wiley-Blackwell. https://doi.org/10 .1002/9781118945582.ch15.

Wipfler, B., Kočárek, P., Richter, A., Boudinot, B., Bai, M. & Beutel, R.G. (2019a) Structural features and life habits of †Alienoptera (Polyneoptera, Dictyoptera, Insecta). *Palaeoentomology*, **2**, 465–473. https://doi.org/10.11646/palaeoentomology.2.5.10.

Wipfler, B., Letsch, H., Frandsen, P.B. *et al.* (2019b) Evolutionary history of Polyneoptera and its implications for our understanding of early winged insects. *Proceedings of the National Academy of Sciences*, **116**, 3024–3029. https://doi.org/10.1073/pnas .1817794116.

Wootton, R.J. (1979) Function, homology and terminology in insect wings. *Systematic Entomology*, **4**, 81–93. https://doi.org/10.1111/j .1365-3113.1979.tb00614.x.

Yager, D.D. & Svenson, G.J. (2008) Patterns of praying mantis auditory system evolution based on morphological, molecular, neurophysiological, and behavioural data. *Biological Journal of the Linnean Society*, **94**, 541–568. https://doi.org/10.1111/j.1095-8312 .2008.00996.x.

Zhang, Z., Schneider, J.W. & Hong, Y. (2013) The most ancient roach (Blattodea): a new genus and species from the earliest Late Carboniferous (Namurian) of China, with a discussion of the phylomorphogeny of early blattids. *Journal of Systematic Palaeontology*, **11**, 27–40. https://doi.org/10.1080/14772019.2011.634443.